AD-A033 493 CIVIL ENGINEERING LAB (NAVY) PORT HUENEME CALIF F/G 8/11
AN EARTHQUAKE ANALYSIS OF THE LIQUEFACTION POTENTIAL AT THE NAV--ETC(U)
SEP 76 J FORREST, J FERRITTO

UNCLASSIFIED CEL-TR-847 NL

1 OF 1
AD
A033493

END

DATE
FILMED
2-77

Technical Report

R847

Sponsored by

NAVAL FACILITIES ENGINEERING COMMAND

September 1976

CIVIL ENGINEERING LABORATORY
Naval Construction Battalion Center
Port Hueneme, California 93043

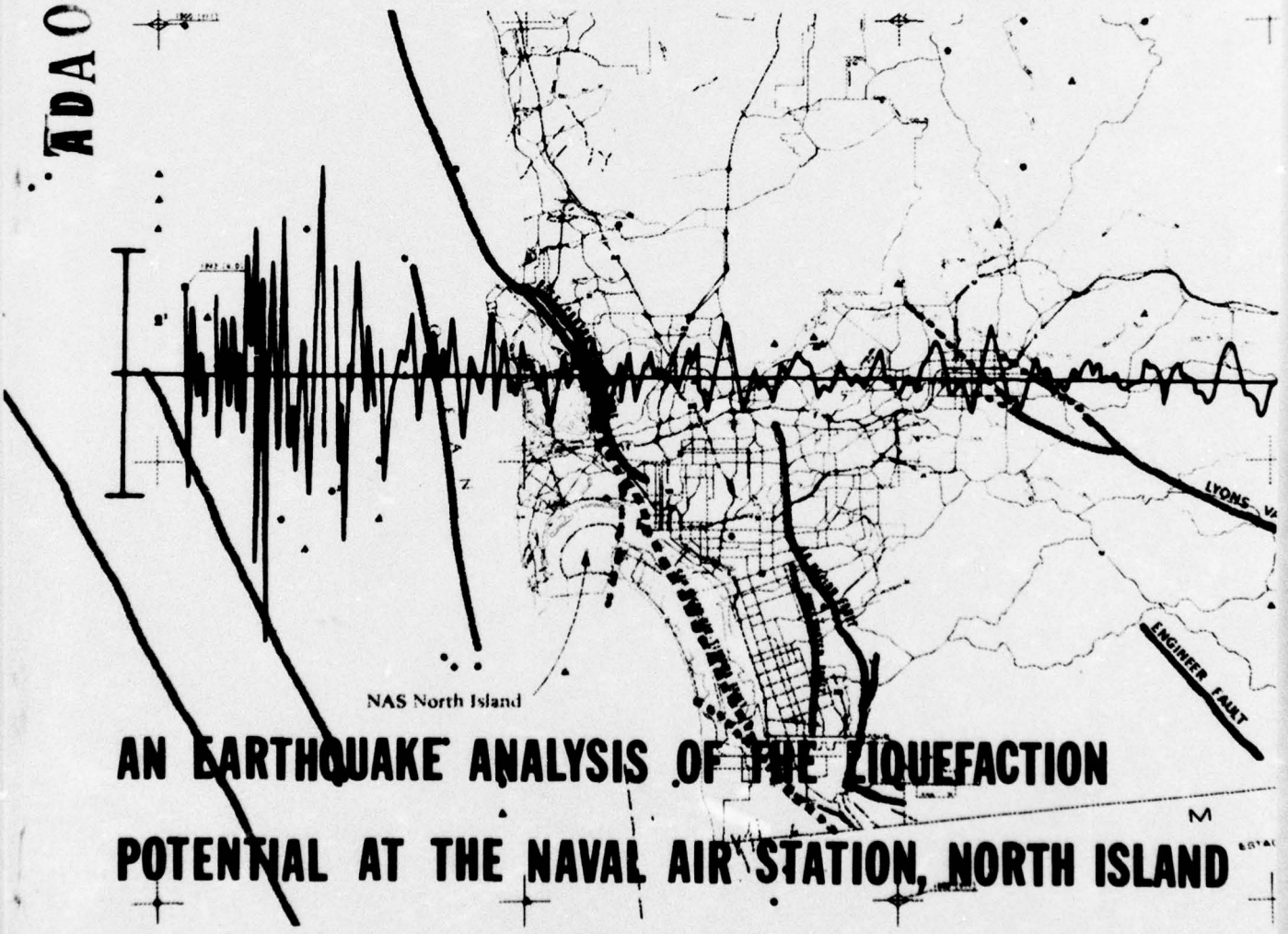

AN EARTHQUAKE ANALYSIS OF THE LIQUEFACTION POTENTIAL AT THE NAVAL AIR STATION, NORTH ISLAND

by J. Forrest and J. Ferritto

Unclassified

SECURITY CLASSIFICATION OF THIS PAGE (When Data Entered)

REPORT DOCUMENTATION PAGE		READ INSTRUCTIONS BEFORE COMPLETING FORM
1. REPORT NUMBER TR-847	2. GOVT ACCESSION NO. DN587105	3. RECIPIENT'S CATALOG NUMBER
4. TITLE (and Subtitle) AN EARTHQUAKE ANALYSIS OF THE LIQUEFACTION POTENTIAL AT THE NAVAL AIR STATION, NORTH ISLAND		5. TYPE OF REPORT & PERIOD COVERED Final; July 1974 – Aug 1975 6. PERFORMING ORG. REPORT NUMBER
7. AUTHOR(s) J. Forrest and J. Ferritto		8. CONTRACT OR GRANT NUMBER(s)
9. PERFORMING ORGANIZATION NAME AND ADDRESS Civil Engineering Laboratory Naval Construction Battalion Center Port Hueneme, California 93043		10. PROGRAM ELEMENT, PROJECT, TASK AREA & WORK UNIT NUMBERS O&M, N; 53-026
11. CONTROLLING OFFICE NAME AND ADDRESS Naval Facilities Engineering Command Alexandria, Virginia 22332		12. REPORT DATE September 1976 13. NUMBER OF PAGES 61
14. MONITORING AGENCY NAME & ADDRESS (if different from Controlling Office) Final rept. Jul 74 – Aug 75,		15. SECURITY CLASS. (of this report) Unclassified 15a. DECLASSIFICATION/DOWNGRADING SCHEDULE
16. DISTRIBUTION STATEMENT (of this Report) Approved for public release; distribution unlimited.		12 68p.
17. DISTRIBUTION STATEMENT (of the abstract entered in Block 20, if different from Report) 14 CEL-TR-847		
18. SUPPLEMENTARY NOTES		
19. KEY WORDS (Continue on reverse side if necessary and identify by block number) Earthquakes, liquefaction, cohesionless soils, ground motions, accelerogram, shear stress, hazards.		
20. ABSTRACT (Continue on reverse side if necessary and identify by block number) The loss of strength experienced by saturated cohesionless soils during earthquake or shock loading is generally referred to as liquefaction. The hazard potential existing at Naval Air Station, North Island, California, due to this phenomenon is evaluated herein, including both a statistical evaluation of potential earthquake levels and an appraisal of the magnitudes of damage. Knowledge of the in-situ soils was used in conjunction with continued		

CONT ON NEXT P.

DD FORM 1 JAN 73 1473 EDITION OF 1 NOV 65 IS OBSOLETE

Unclassified

SECURITY CLASSIFICATION OF THIS PAGE (When Data Entered)

391 111

AB

20. Continued

earthquake-response predictions in the most recent state-of-the-art prediction procedures. Problems encountered in making liquefaction evaluations are discussed in some detail. These problems include predicting the magnitude and recurrence rates (frequency) of ground motions to be expected, determining the true nature of the subsurface soils, and finally evaluating the effect of the applied ground motions on these subsurface soils.

This report concludes that although most of North Island is underlain by natural sands which should be fairly resistant to liquefaction, limited regions with very high liquefaction potential exist. These regions would be expected to liquefy under earthquake levels used for engineering analysis, and present a high damage potential to such critical structures as the carrier docking facilities, aviation fuel tank farms, and service lines.

Library Card

Civil Engineering Laboratory
AN EARTHQUAKE ANALYSIS OF THE LIQUEFACTION POTENTIAL AT THE NAVAL AIR STATION, NORTH ISLAND (Final), by J. Forrest and J. Ferritto
TR-847 61 pp illus September 1976 Unclassified

1. Earthquake loading 2. Liquefaction I. 53-026

Loss of strength experienced by saturated cohesionless soils during earthquake loading is referred to as liquefaction. This hazard potential at Naval Air Station, North Island, California, is evaluated in a statistical evaluation of earthquakes potentials and an appraisal of the magnitudes of damage. Knowledge of in-situ soils was used in conjunction with earthquake-response predictions. Problems in making liquefaction evaluations are discussed. Predictions of the magnitude and recurrence rates (frequency) of ground motions to be expected, determinations of the true nature of the subsurface soils, and evaluations of the effect of the applied ground motions on these subsurface soils are made. It is concluded that most of North Island should be fairly resistant to liquefaction, but limited regions with very high liquefaction potential exist. These regions would present a high damage potential to critical facilities.

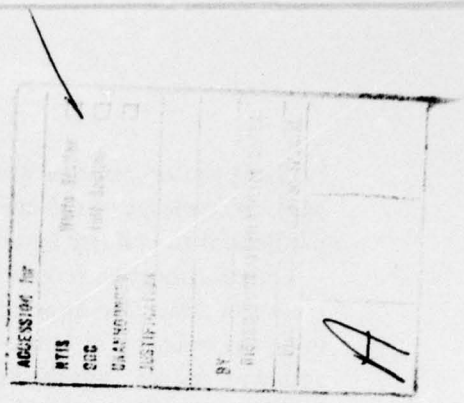

INTRODUCTION

Catastrophes have occurred world wide because of liquefaction of saturated sandy soils when the ground is shaken during an earthquake. This liquefaction has been responsible for such things as settlement and tilting of buildings, failure of waterfront retaining structures, lateral movement of bridge supports, and major landslides.

Liquefaction describes a phenomenon in which a saturated cohesionless soil loses its strength during an earthquake or under shock-loading, and acquires a degree of mobility sufficient to permit soil movements ranging from a few feet up to many feet.

A recent study by an Office of Naval Research (ONR) Natural Hazards Review Panel [1] assessing the potential of major earthquake damage has suggested that a considerable earthquake threat exists at Naval Air Station (NAS) North Island, California. The panel estimated that the earthquake threat included the possibility of magnitude 7 or greater earthquakes occurring within 15 miles of NAS North Island and even suggested the possibility of a major earthquake occurring on a possible major fault passing through San Diego Bay itself. It was estimated that such earthquakes could result in ground accelerations at NAS North Island in excess of 0.3 g. Based upon experience at Niigata, Japan, the predicted possible ground accelerations could cause liquefaction in the North Island uniform sands whenever the relative density of sand approaches 50% or less. Such cyclic instability in the soil at NAS North Island would be expected to cause severe damage to such structures as fuel storage tanks, carrier mooring berths, water and sewer lines, and some buildings.

As a result of the ONR study, the Naval Facilities Engineering Command (NAVFAC) tasked the Civil Engineering Laboratory (CEL) to perform a more detailed investigation of the liquefaction potential at NAS North Island. The principal objectives were:

1. To provide a statistical evaluation of the earthquake potential at NAS North Island

2. To appraise the threat of soil liquefaction during such an earthquake and

3. To develop optimized or improved procedures for analyzing the hazards of earthquake-induced soil liquefaction at naval shore facilities.

Existing soil data were assembled—enhanced by additional field investigations—to define the soil profile existing at NAS North Island. Seismological records and

available geologic studies were used to evaluate potential earthquake ground-motion levels. Knowledge of the in-situ soils were used in conjunction with earthquake-response predictions to evaluate liquefaction potentials throughout NAS North Island.

Liquefaction occurs only in saturated cohesionless materials such as sands below the water table. The liquefaction potential under cyclic loading depends primarily upon the intensity and duration of shaking, the relative density and confining stresses acting on the soil, and the drainage conditions; (i.e., permeability and boundaries of soil deposits). Thus, with the density, location, and characteristics of the various cohesionless soils at NAS North Island and the predicted ground motions known, areas in danger of liquefaction can be determined.

This study assembled existing soil data on NAS North Island, with particular regard to material type and density. Seismological and geological studies were consulted to provide information on expected earthquake magnitudes. In particular, the earthquake level with a 10% probability of being exceeded over a 25-year period was considered. The most critical areas at NAS North Island were defined by the current methods of appraising liquefaction potential. Problems encountered in making estimates of liquefaction hazards at North Island are discussed and serve to suggest additional improvements necessary to provide an efficient procedure for evaluating earthquake hazards at other naval shore facilities.

SITE DESCRIPTION

NAS North Island occupies about 2,580 acres of land and constitutes the major portion of Coronado Island, situated between San Diego Bay and the Pacific Ocean at San Diego, California. Portions of the air station were below sea level and have been reclaimed by placing hydraulic fill—primarily sands—dredged from the bottom of San Diego Bay. Reclaimed areas (see Figure 1) include: (1)the former Spanish Bight, near the east boundary of the station; (2) Whaler's Bight, near the southwest extremity of the property; and (3) a strip of land along the northwest beachline. Spanish Bight was filled in 1945. The other two areas, and the surrounding beaches in general, have been subjected to numerous cycles of filling and erosion but were primarily completed in stages between 1919 and 1952. The North Island facility was originally established in 1938 as a seaplane base. Construction has continued to the present, but the last major airfield construction took place in 1961.

Geology

North Island is located on a narrow northwest-trending coastal plane, a natural geomorphic province known as the coastal plane of Southern California. Basement rocks beneath the area are the California batholith of Cretaceous time and peak volcanics of the Jurassic era [2, 3]. Post-batholith rocks of the coastal plane are mainly clastic

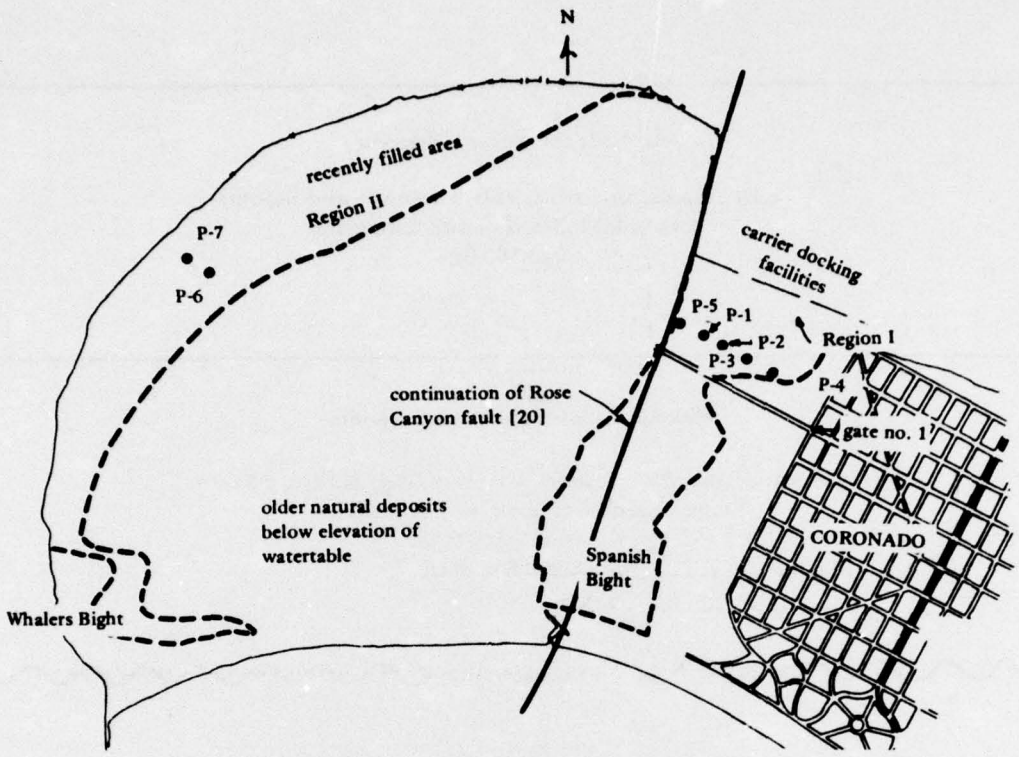

Figure 1. Recently filled areas and soil-boring locations at NAS North Island.

marine sedimentary deposits that cover the older rocks and commonly dip gently toward the west and southwest [3]. These rocks range in age from Cretaceous to Quaternary and consist chiefly of beds of sandstone, shale and conglomerate. Prominent structural features include numerous and extensive northwest-trending faults throughout the area. Fault descriptions are discussed in more detail in later sections of this report.

Pleistocene terrace deposits of marine and nonmarine origin exist along the coasts near San Diego, overlying sedimentary Eocene and Pliocene sedimentary rocks. These terrace deposits range from poorly consolidated, poorly sorted silts to gravels. Prominent among these is the Linda Vista formation, a reddish brown marine deposit containing iron oxide. Recent alluvial deposits at the site include clay-size through gravels. These materials are unconsolidated and are made up of various granite and metamorphic rock types. A simplified geologic profile is shown in Figure 2 [2, 3, 4].

Soil Profile

The soil profile at NAS North Island was studied using the results of approximately 60 previous building foundation investigations carried out under the authority of Western Division, NAVFAC, San Bruno, California. The numbers on Figure 3 show the locations of previous foundation investigations and are identified in the Appendix. Available

Figure 2. Simplified geologic profile at NAS North Island.

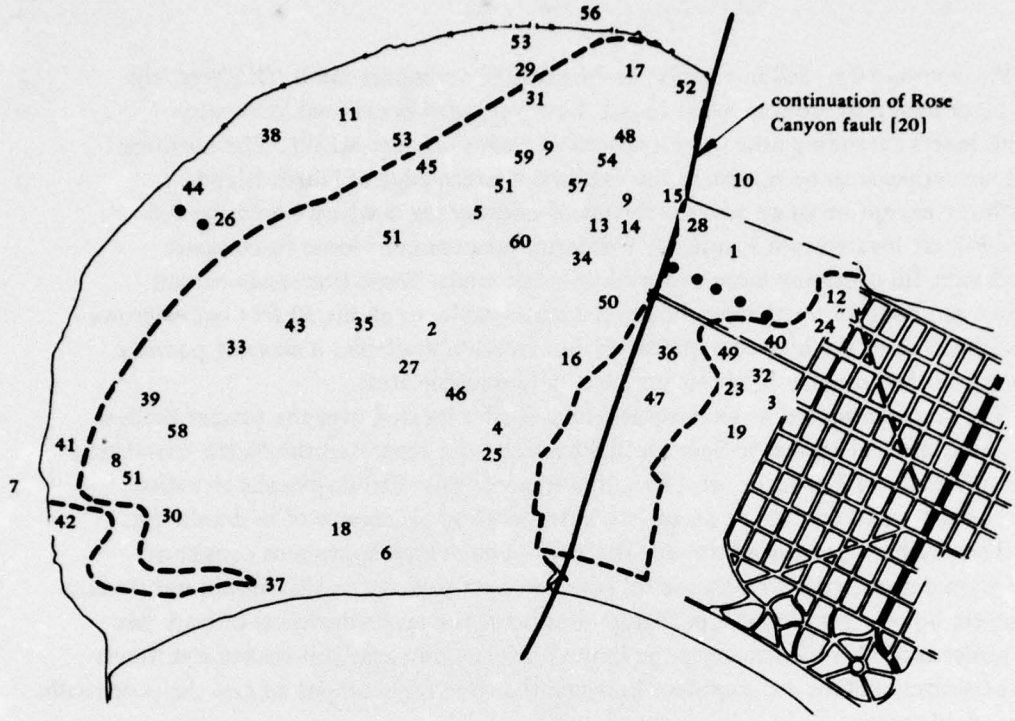

Figure 3. Locations of previously conducted foundation investigations.

data were supplemented by additional soil borings and static cone penetrometer soundings [5] to depths as much as 30 feet in two of the hydraulically filled areas. The locations of the supplementary borings (P1-P7) are shown in Figure 1. Available information from the previous foundation investigations suggests that the older, naturally deposited portions of North Island would be relatively resistant to liquefaction. These areas make up the central portion of the air station and a small region just east of the former Spanish Bight (near Gate 1, the McCain Avenue entrance).

The central portion of the island contains some loose fill and rubble, but appears to have only medium dense to very dense* native materials at elevations below that of the water table. The soil profile for the older portion of the air station near gate no. 1 is similar to that of the central areas. These relatively competent areas are separated by a region which includes thin strata of loose deposits at depths beneath the water table, located about 10 feet below the surface in this region. The entire North Island area appears to contain primarily dense materials below elevation -20 feet mean low water level (MLWL). The filled area in the extreme west (Figure 1) contains loose materials near the ground surface, with some organic material in the vicinity of Whaler's Bight. Below the elevation of the ground water table (about 6.0 feet MLWL in this area) in-situ materials are extremely variable

*Standard penetration test blow counts of 30 to 100.

(blow counts 10 to 50) but appear to be primarily compact sands. Offshore, the in-place materials are somewhat looser, however, with occasional loose silty sand layers extending down to elevations of about -25 feet MLWL. The northern fill area appears to be similar to the extreme western edge of North Island with the exception of an area northwest of taxiway no. 5 where boreholes P-6 and P-7 are located (see Figure 1). This latter area contains loose-to-compact hydraulic fill overlying loose-to-very-loose fine sands. These fine sands extend down to about 15 feet below the ground water table, or about 30 feet below ground surface. Due to the limited exploratory information available, it was not possible to define the boundaries of this potentially liquefiable area.

The area considered to be most critical was that located over the former shallow bay-like channel known as Spanish Bight which once separated the North Island area from the city of Coronado. In 1945, this area was raised to its present elevation of about 8 to 12 feet above mean low water level by placement of hydraulic fill.

The southern portion of the Spanish Bight area, which appears to consist of medium dense dredged hydraulic fill over compact to dense sands, should not present a severe liquefaction hazard, probably because of the lesser thickness of both bay deposits and fill. Unfortunately the limited information available makes it difficult to accurately define the boundary between the relatively competent and the potentially liquefiable areas.

It is the northern portion of the Spanish Bight area where the potential for liquefaction appears highest. This region, particularly along the eastern edge of the former bight but widening to the north, appears to include a considerable thickness of soft bay deposits.

Available foundation investigation data for this region showed that in measurements of penetration resistance, made by standard penetration tests (SPT) [6], as low as one blow of a 140-pound hammer falling 30 inches, was required to drive the standard sampler 12 inches. This indicates extremely soft or loose deposits. Also, very low values of in-situ density had been determined from recovered drive samples. Many of these soft materials were identified as fine sands and silts with negligible plasticity. Thus, based upon the available information, in-situ materials in the former Spanish Bight area appeared to be unusually loose, cohesionless, fine sands. The very low blow counts however, raised the possibility that either the soft layers were not cohesionless or, due to their high sensitivity, were liquefying during driving of the sampler.

Since cohesive materials do not exhibit the type of liquefaction of interest herein, it was critical that the true nature of this material be ascertained. It is also conceivable that a sensitive material could have a degree of cementation and would liquefy under the shock of a drive sampler, yet maintain its integrity under the levels of dynamic loading that would be experienced during an earthquake.

In an attempt to obtain more reliable information on the undisturbed nature of the in-situ soils, a static cone penetrometer or friction cone was used [5].

Seven penetration holes were made, five in the former Spanish Bight area, and holes P-6 and P-7 in the filled area along the western perimeter of North Island (see Figure 1).

The cone penetrometer tests provide values of the penetration resistance encountered while pushing a standard shaped cone (60-degree angle and 10 cm^2 cross section area) into the soil at a rate of 2 cm/sec. Separate readings of point resistance and the resistance due to side friction along a standard sleeve and obtained at increments of 20 cm. Based upon the ratio of side friction along the sleeve segment to the point resistance (friction ratio), the type of material encountered can be evaluated [7]. The absolute value of point resistance provides an indication of the competency or load-carrying capacity of the soil [8]. Cone penetrometer readings for 30-foot probings at the seven locations are shown in Figure 4. Various correlations exist between cone penetrometer resistance and relative density. A typical relationship between penetration resistance as proposed by Meyerhof [9] is shown in Table 1. These correlations, together with the information in Figure 4, indicate that extremely loose or soft deposits are present within approximately the upper 20 feet of the Spanish Bight area. The materials found in holes P-6 and P-7 at the western extremity of the Naval Air Station are also very soft, or loose, to depths of about 25 feet but appear to be slightly more competent (i.e. higher penetration resistances) than the Spanish Bight soils. Reference to the friction ratios of Figure 4 suggests that many of these very weak soils are of a noncohesive nature. This information reinforces the available dynamic penetration data, suggesting unreasonably loose cohesionless soil layers at various depths beneath the water table. Should liquefaction be occurring during the quasi-static cone penetration test, then the situation is probably more critical than that indicated by liquefaction under dynamic drive sampling. It was felt that an alternative cause for the extremely low penetration values (i.e., the possible presence of soft plastic soils) must be investigated: the possibility that the area included numerous interbedded layers of soft clays and sands, with the soft clay layers responsible for the very low penetration values.

To investigate this possibility required samples from the locations of low cone penetrometer resistance. A hollow stem auger was used to drill holes at locations within 1 or 2 feet of the sites where the penetrometer data were obtained. At regions of minimal soil support, continuous sampling was carried out through the auger stem using a California drive sampler, which is similar to the standard split spoon [6] but with a 2-1/2-inch diameter. Penetrometer readings were recorded, and samples were taken for classification in the CEL soils laboratory. The number of blows recorded while driving the dynamic penetrometer are also shown in Figure 4. A generalized soil profile was developed based upon the results of the friction cone tests, the standard drilling and sampling investigation, and the results of the laboratory tests. Figure 5 shows a simplified soil profile representing a section across the former Spanish Bight (boreholes P-1 to P-5).

Table 1. Relationship Between Relative Density and Penetration Resistance for Cohesionless Soils [9].

State of Packing	Relative Density	Standard Penetration Resistance (blows/ft)	Static Cone Resistance (tons/ft^2)
Very loose	< 0.2	< 4	< 20
Loose	0.2 - 0.4	4 - 10	20 - 40
Compact	0.4 - 0.6	10 - 30	40 - 120
Dense	0.6 - 0.8	30 - 50	120 - 200
Very dense	> 0.8	> 50	> 200

The actual soil profile was extremely heterogeneous with many thin interbedded clay, silt, and sand layers. Large accumulations of shells were noted at some locations. The profile of Figure 5 represents an attempt to provide an equivalent, average cross section. The surface soils, apparently dredged fill, contain extremely high percentages of mica (muscovite) in some locations. The upper sands have been compacted to a high density just beneath the surface. They appear to grade into a very highly micaceous silty layer overlaying a silty clay at about the water table (3 feet MLWL). This silty region (designated layer 2 in Figure 5) contained layers of extremely high mica content alternating with darker siltier bands, giving the appearance of the "varved" clays observed in formerly glaciated regions [10].

The clay layer (layer 3) appeared to be near the "A" line that divides silts from clays in the Unified Classification System [10]. This layer extended from low to high plasticity, with moisture content up to 96%. This probably represents the surface of the former bay deposits. Layers 4 and 5 (bay deposits) appeared to be an extremely sensitive silty sand with occasional silt layers. Unfortunately, it was impossible to obtain samples from the lower elevations of layer 5 with the available equipment. Many of the samples obtained from layer 5 had a rather resilient cemented structure when taken from the sampling tube, but became completely nonplastic when remolded for Atterberg limits tests. Below the silty layers the materials of layer 6 were primarily silty medium sands of relatively high density to the depths investigated.

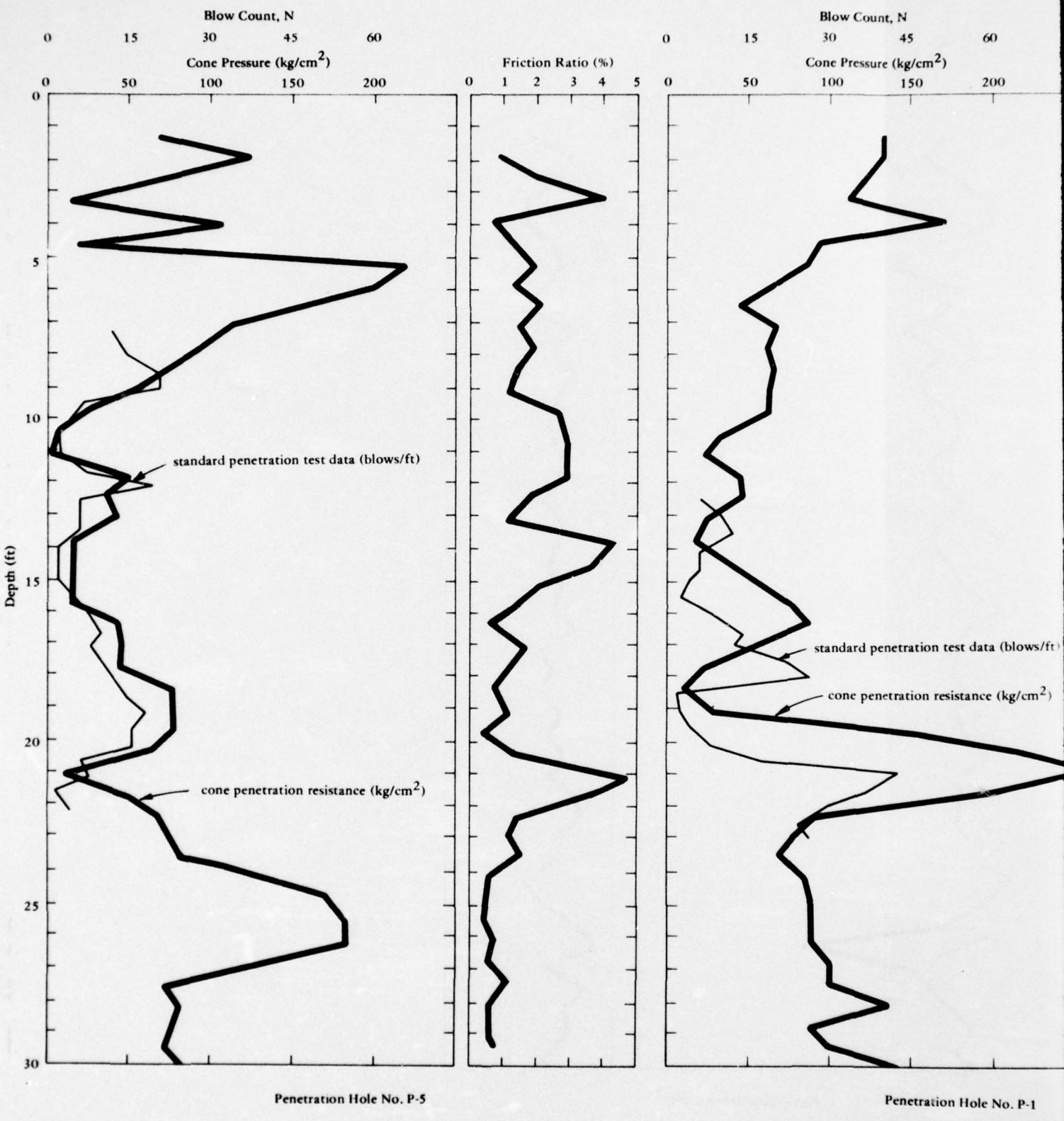
Blow Count, N
0 15 30 45 60
Cone Pressure (kg/cm²)
0 50 100 150 200
Friction Ratio (%)
0 1 2 3 4 5
Depth (ft)
0 5 10 15 20 25 30
standard penetration test data (blows/ft)
cone penetration resistance (kg/cm²)
Penetration Hole No. P-5
Blow Count, N
0 15 30 45 60
Cone Pressure (kg/cm²)
0 50 100 150 200
standard penetration test data (blows/ft)
cone penetration resistance (kg/cm²)
Penetration Hole No. P-1

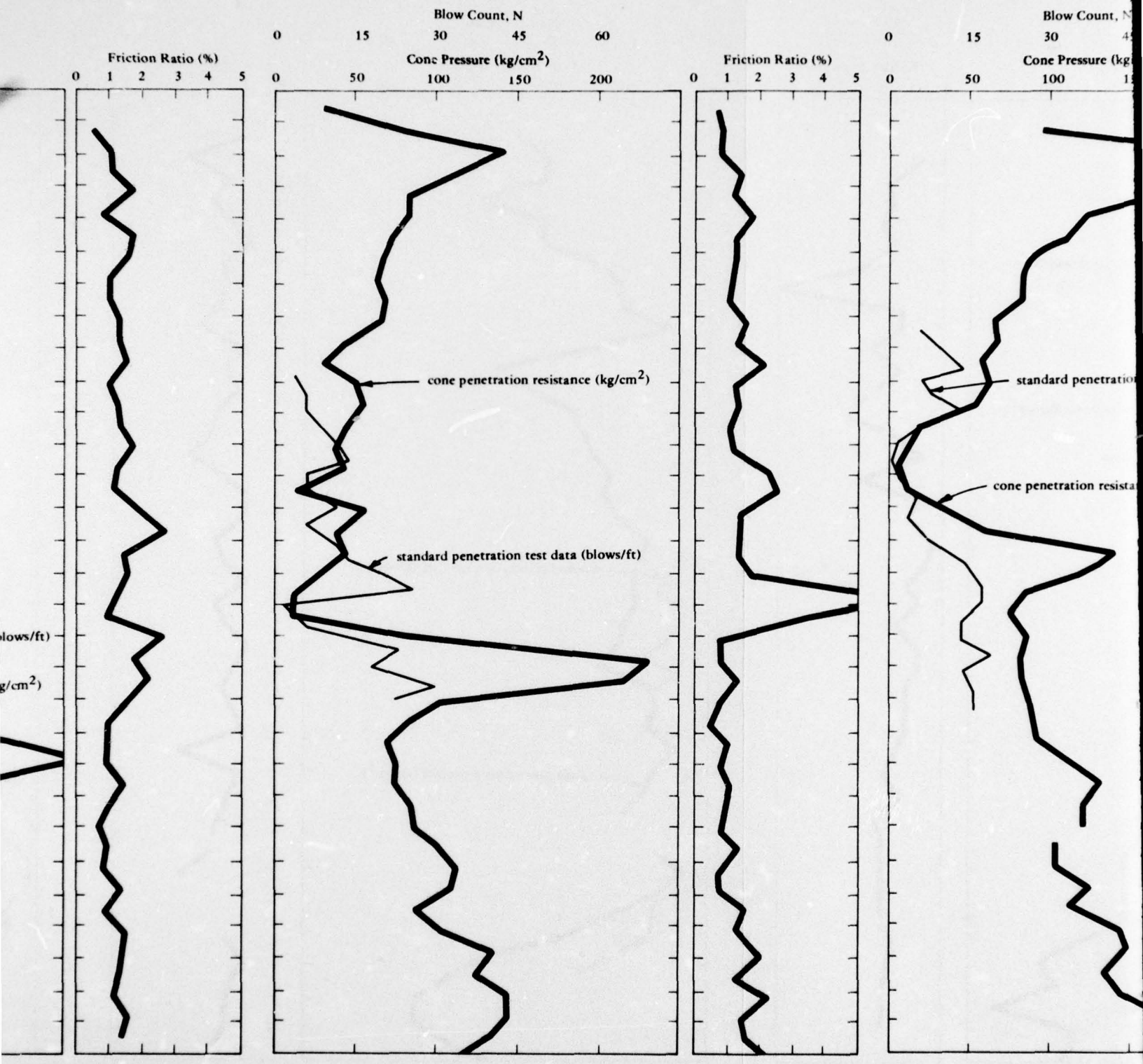

Figure 4. Soil exploratory data.

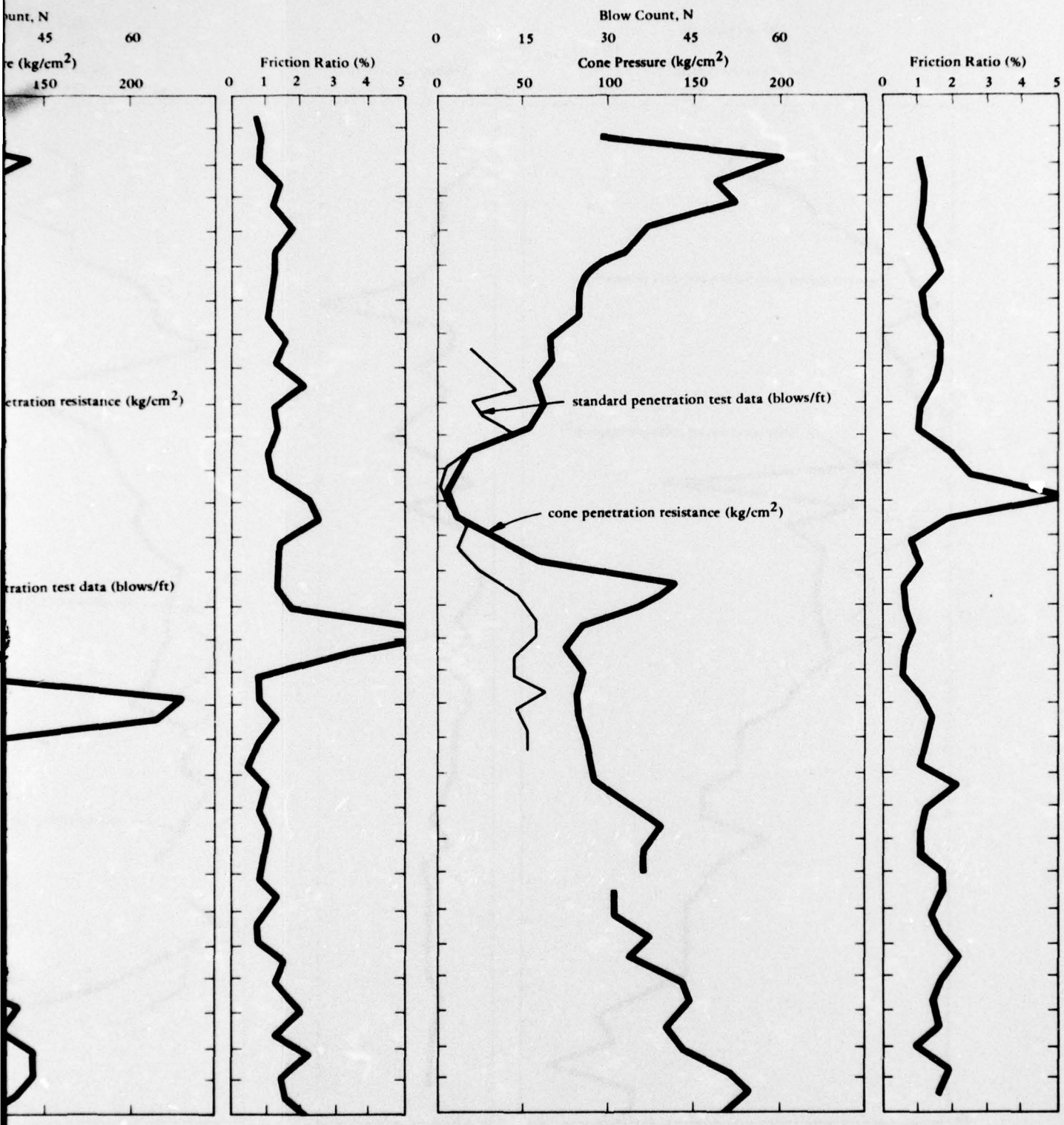

Penetration Hole No. P-2

Penetration Hole No. P-3

3

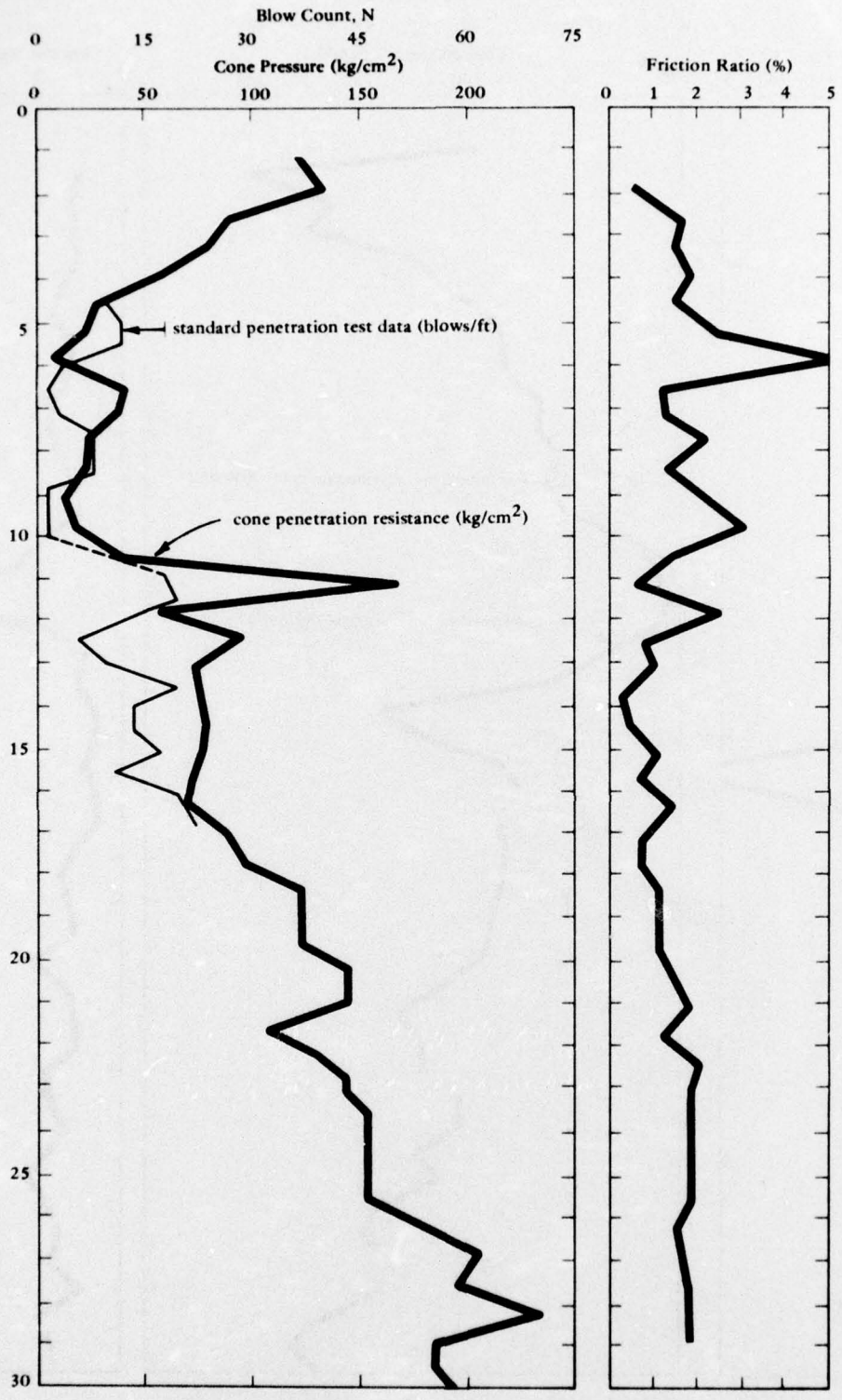
Blow Count, N
0
15
30
45
60
75
Cone Pressure (kg/cm2)
0
50
100
150
200
Friction Ratio (%)
0
1
2
3
4
5
0
5
10
15
20
25
30
standard penetration test data (blows/ft)
cone penetration resistance (kg/cm2)
Penetration Hole No. P-4

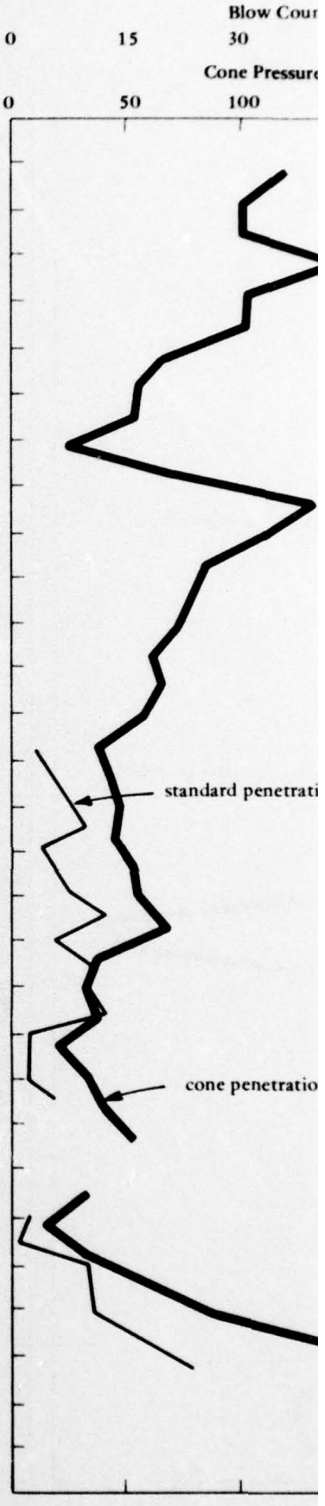
Blow Coun
0
15
30
Cone Pressure
0
50
100
standard penetrati
cone penetratio

Figure 4.

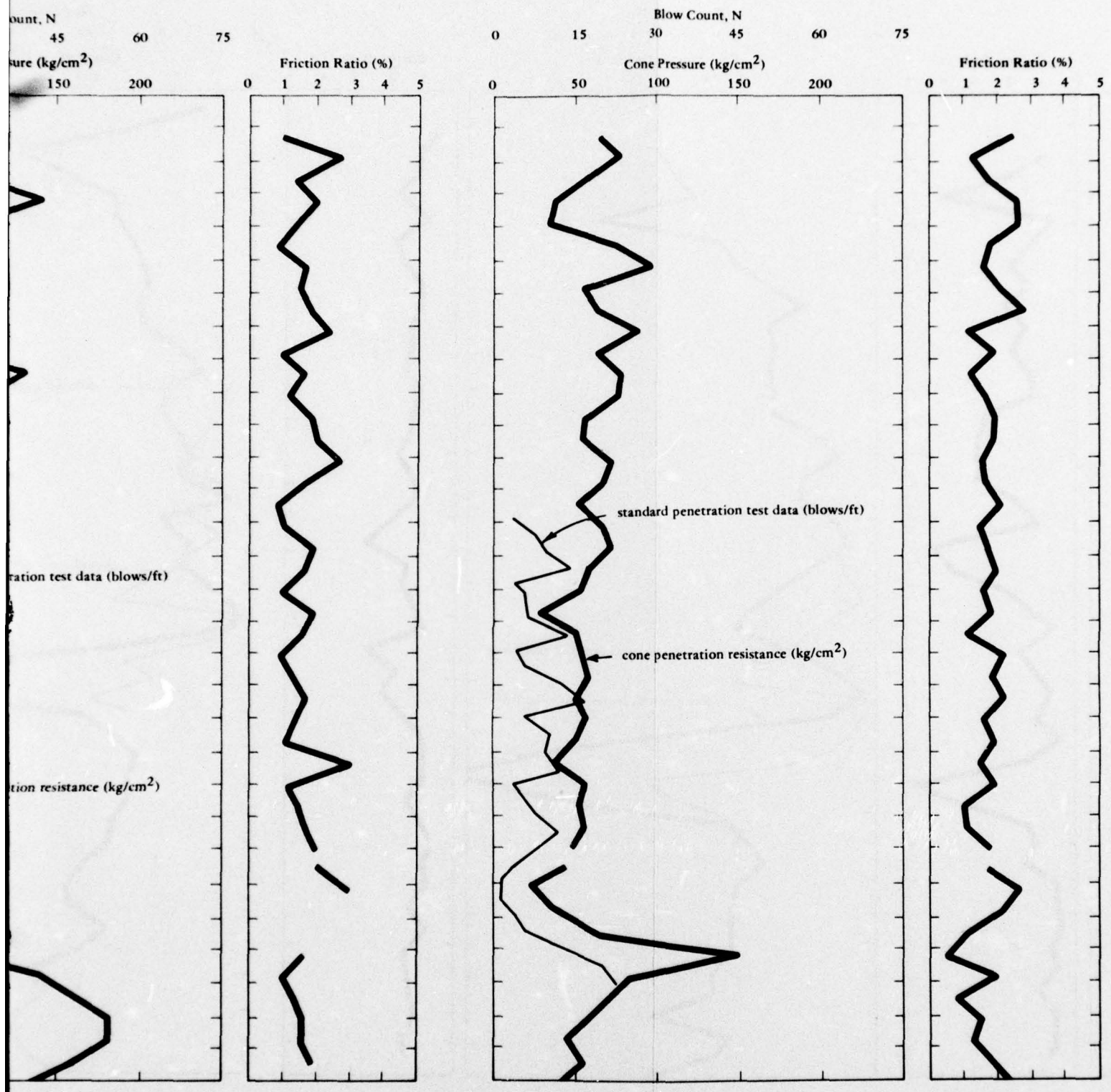
ount, N
45
60
75
sure (kg/cm²)
150
200
ration test data (blows/ft)
tion resistance (kg/cm²)
Friction Ratio (%)
0
1
2
3
4
5
Penetration Hole No. P-6
Blow Count, N
0
15
30
45
60
75
Cone Pressure (kg/cm²)
0
50
100
150
200
standard penetration test data (blows/ft)
cone penetration resistance (kg/cm²)
Friction Ratio (%)
0
1
2
3
4
5
Penetration Hole No. P-7

4. Continued

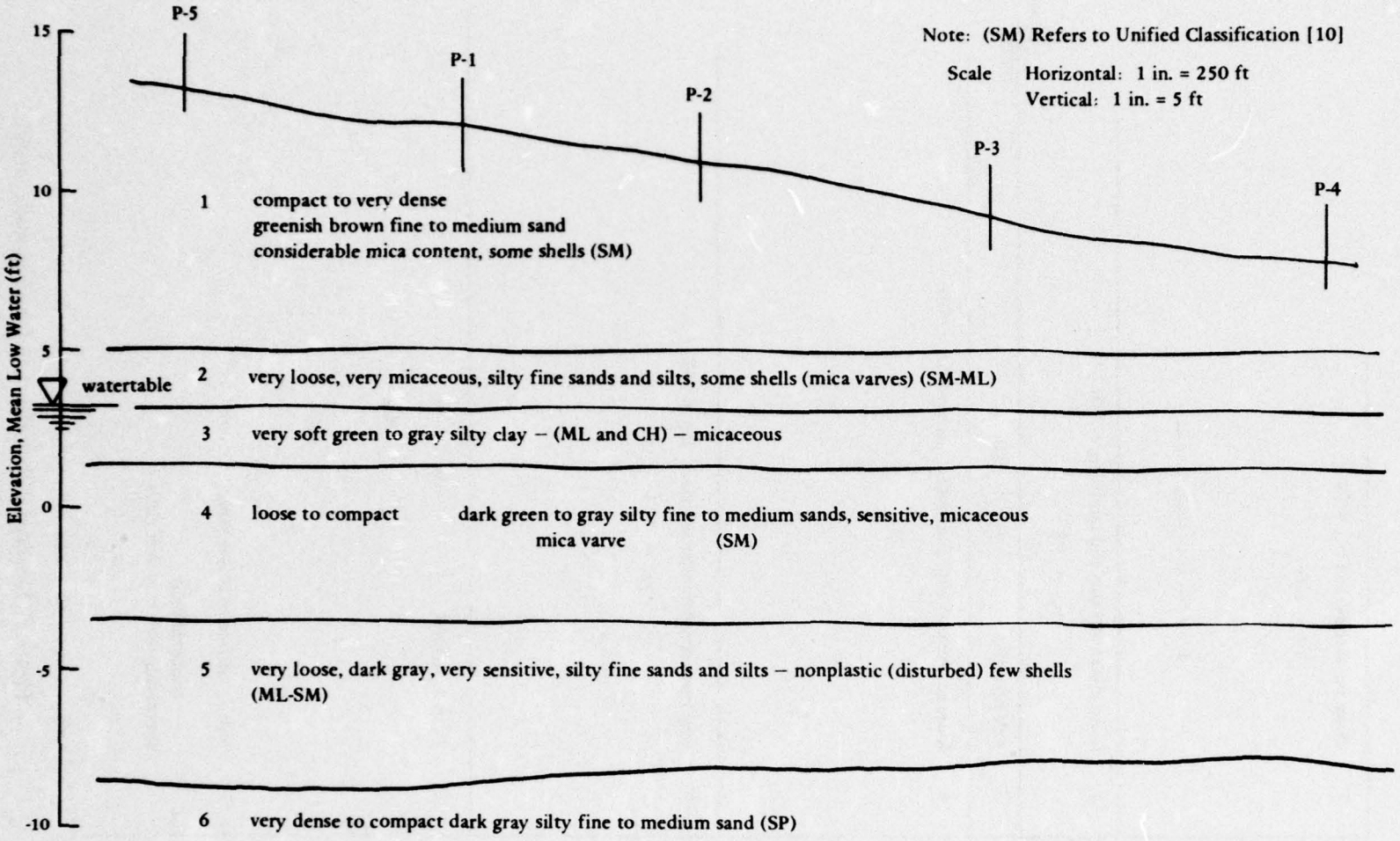

Figure 5. Generalized soil profile across former Spanish Bight.

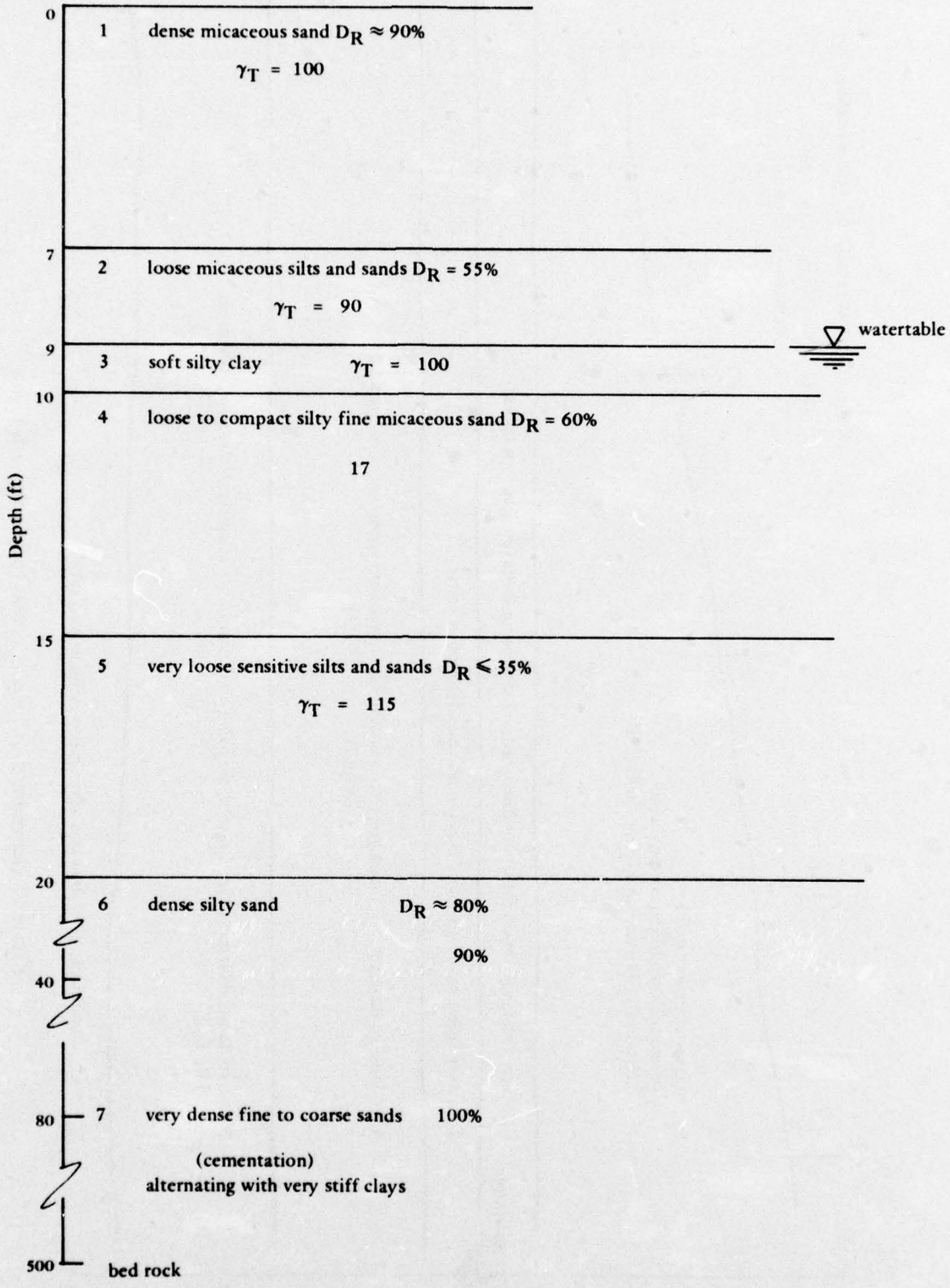

Figure 6. Idealized soil profile used for earthquake analysis.

Based upon available information, the idealized profile of Figure 6 was adopted for ground-motion analysis. Unfortunately the peculiar materials at this site, specifically the micaceous silty fine sands and the sensitive sandy silts are not typical soil materials. To determine how the extremely high mica contents influence the dynamic behavior of the in-situ materials would require a testing program that is beyond the scope of this project. It is apparent that drive samples of the very sensitive silty materials could undergo major disturbances during their acquisition. The response of such samples in the laboratory might differ greatly from the in-situ response of the material in an undisturbed state.

On a simpler level, merely estimating soil density for such soils on the basis of either dynamic or static penetration readings could introduce major inaccuracies. Maximum and minimum densities obtained in the laboratory for the North Island materials were noted to be considerably below those for typical soils (see Figure 7). Thus, any correlations used to predict relative density or void ratio and, hence, strength and stiffness, of the North Island soils on the basis of penetration resistance could be greatly in error.

EARTHQUAKE ACTIVITY FOR ENGINEERING ANALYSIS

Seismicity

The seismicity and regional geologic structure of the San Diego area can be interpreted in the light of current plate tectonic theory. California is believed to lie on the junction of two relatively rigid plates of the earth's crust which respond to movement of subcrustal material. The main evidence of this juncture is the San Andreas Fault [11, 12]. These same forces that tend to move the portion of California on the westerly side of the San Andreas fault northward have resulted in the formation of other faults such as the San Jacinto, Whittier-Elsinore and Newport-Inglewood. General major faulting in the San Diego region is shown in Figure 8 [13].

Earthquakes occur in areas where the differential stress exceeds the shearing resistance of the material in the area, resulting in rupture. Regions of differential strain exist around faults. The information used in an earthquake engineering analysis includes identification and delineation of those faults that are active—that is, capable of generating earthquakes.

For specific land uses, information about recency of faulting is useful in designating particular faults as active. It is assumed that the more recent the faulting the more likely it is that the fault will undergo intermittent displacement in the geologically near future. Movement is presumed less likely to occur along faults that have progressively longer periods of demonstrated quiescence. Because of the apparent great range in frequency of movement, no agreement has been reached at present on the length of geologic time pertinent for evaluating the near-future behavior of faults. Selection of the timespan used to designate faults as active based

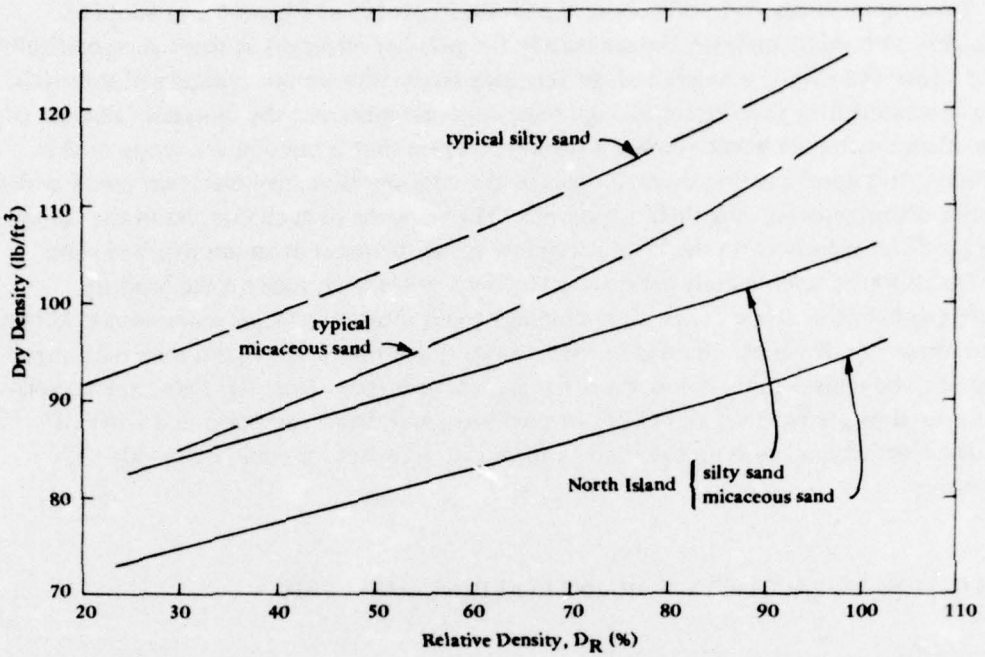

Figure 7. Dry density versus relative density relationships.

on the age of latest movement has been influenced by the potential consequence of seismic shaking or surface faulting on a specific structure. The greater the risk to be incurred, the longer the timespan that must be considered. Displacement during Holocene time (the past 11,000 years) is a generally accepted criterion of activity for many land uses. This timespan is probably inadequate, however, to assure recognition of all active faults [13]. Historic offsets have occurred along faults, such as the White Wolf fault, that had not previously shown recognized evidence of Holocene faulting. Wentworth and Yerkes [14] state that evidence of displacement during late Quaternary time (the past several hundred thousand years) should be considered evidence that a fault is probably active.

The U.S. Atomic Energy Commission requires that faults with movements during the past 500,000 years be considered active for siting and design of nuclear power facilities. The summary of present opinion indicates at least the past few hundred thousand years are important for assessing present activity of a fault. Ziony and Buchanan [15] suggested that faults offsetting lower Pleistocene strata (2 million years) should be considered active in the San Diego area, because these faults commonly have no significant late Quaternary Age (500,000 years) control to preclude younger movement. The last two earthquakes producing extensive damage in southern California—Arvin-Tehachapi, 1952 and San Fernando, 1971—occurred on faults lacking historic activity. Every event greater than magnitude 6 in southern California occurred on a fault (with the exception of the San Jacinto fault system) without prior historic activity.

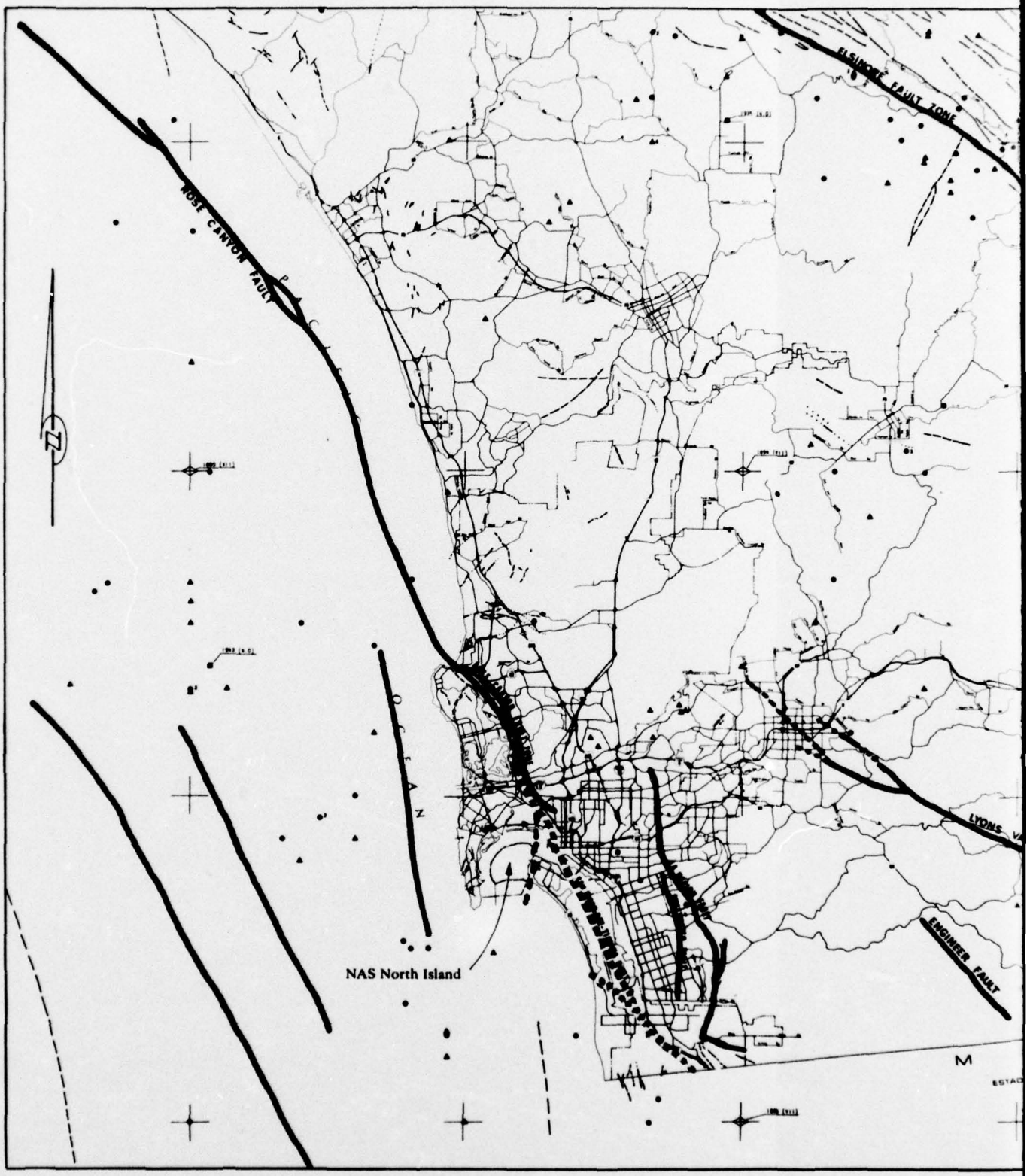

Figure 8. Major faulting in the San Dieg

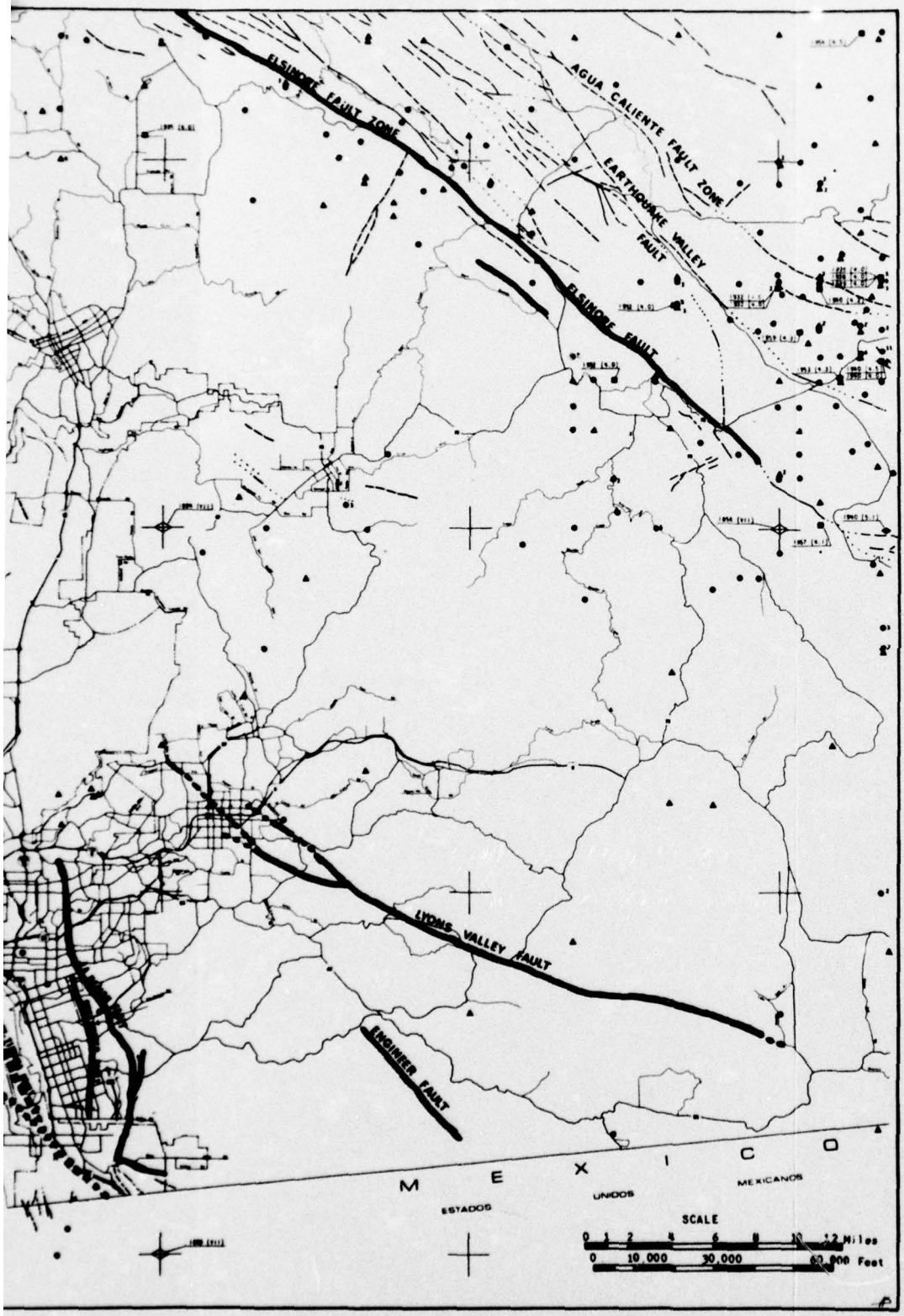

Legend: Faults: ——— (Solid where well defined, dashed where approximate or inferred, dotted where concealed.)

Epicenter Magnitude Ranges: ▲ 2.0-2.9 ● 3.0-3.9 ■ 4.0-4.9 ◆ 5.0-5.9

Epicenter Intensity Ranges: ◇ VI-VII

Figure 8. Major faulting in the San Diego region.

2

Empirical expressions have been developed in References 16, 17, and 18, relating earthquake magnitude, fault length, and offset displacements. Although these relationships can serve as guides, they have inherent weaknesses from uncertainties involved in their development.

The rupture of a fault generates body waves propagating within the earth and surface waves propagating on the surface. The body waves are composed of dilatational waves and distortional or transverse shear waves, both vertical and horizontal. The surface waves are Love waves which involve a surface layer in horizontal transverse vibration and Rayleigh waves which comprise circular vibration in retrograde orbit. Each of these types of waves propagates at its own velocity, and each arrives at specific locations at different times. Shock waves travel fastest through the higher velocity medias at depth (bedrock). The waves tend to be refracted toward the vertical as they propagate upward through increasingly softer materials near the surface. This follows from Snell's law because shallower layers generally have lower wave velocities than deeper layers. Thus, shear waves tend to approach the surface traveling in the vertical direction and vibrating in a horizontal plane. Use of standard safety factors result in most structures being well-designed for vertical loads. However, horizontal shear waves induce motions and load in the structure in the horizontal plane. Strong motion accelerograms show that vertical vibrations are generally only two-thirds as large as horizontal vibrations. For this reason, vertically propagating, horizontal motions are considered of greatest importance, and most work has centered on understanding them.

Rock motions beneath a particular site will depend upon the energy released along the fault (characterized by the magnitude of the earthquake) and upon the distance of the site from the zone of energy release. Table 2 [19] summarizes different attenuation equations developed for ground motions. Figure 9 compares the attenuation equations for a magnitude 6.5 earthquake with measured data for the 1971 San Fernando earthquake. Although site conditions are not defined—other than as soil or rock—it is clear that there is a wide range in predictions of motion at a given distance. Thus, estimation of ground motion is an extremely imperfect procedure resulting in upper and lower bounds differing by as much as 100% from mean predictions.

In developing a ground-motion prediction, it is necessary to define the distance from the point of interest to the fault under consideration. If the fault break is short in length and the site is located a considerable distance from the fault, the significant distance from the site to the zone of energy release can be expressed by the epicentral distance. In the case of a long fault this can be grossly misleading because the rupture of the fault propagates along its length. When the site is close to a fault the distance should reflect the release of energy as the rupture propagates along the fault length. In such a case, the distance to the site from the zone of energy release is more appropriately characterized by the shortest distance to the causative fault rather than the distance to the epicenter [20]. To give perspective to this, consider Table 3 which gives tentative relationships between magnitude and length of fault that has slipped.

Table 2. Attenuation Equations for Ground-Motion Acceleration [19].

Data Source	Equation[a]
1. San Fernando Earthquake February 9, 1971	$y = 186206\ R^{-1.83}$
2. Housner (1965)	Graphical Presentation California Earthquakes
3. California and Japanese Earthquakes	$y = \frac{5}{\sqrt{T_G}}\ 10^{0.61m - P \log R + Q}$ where $P = 1.66 + \frac{3.60}{R}$, $Q = 0.167 - \frac{1.83}{R}$, T_G = fundamental period of site
4. Cloud (1963)	$y = \frac{6.77\ e^{1.64m}}{1.1\ e^{1.1m} + R^2}$
5. Cloud (1963) Housner (1962)	$y = 1230\ e^{0.8m}\ (R + 25)^{-2}$
6. Schnabel and Seed (1973)	Graphical Presentation 11 Selected Records
7. 303 Instrumental Values	$y = 1300\ e^{0.67m}\ (R + 25)^{-1.6}$
8. Western U.S. Records	$y = 18.9\ e^{0.8m}\ (R^2 + 400)^{-1}$
9. Western U.S. Records	$\log_{10}[y] = m + \log_{10} A_o(R) - \log_{10} a_o(m)$

[a] y is cm/sec^2
R is kilometers (distance to causative fault)
m is magnitude

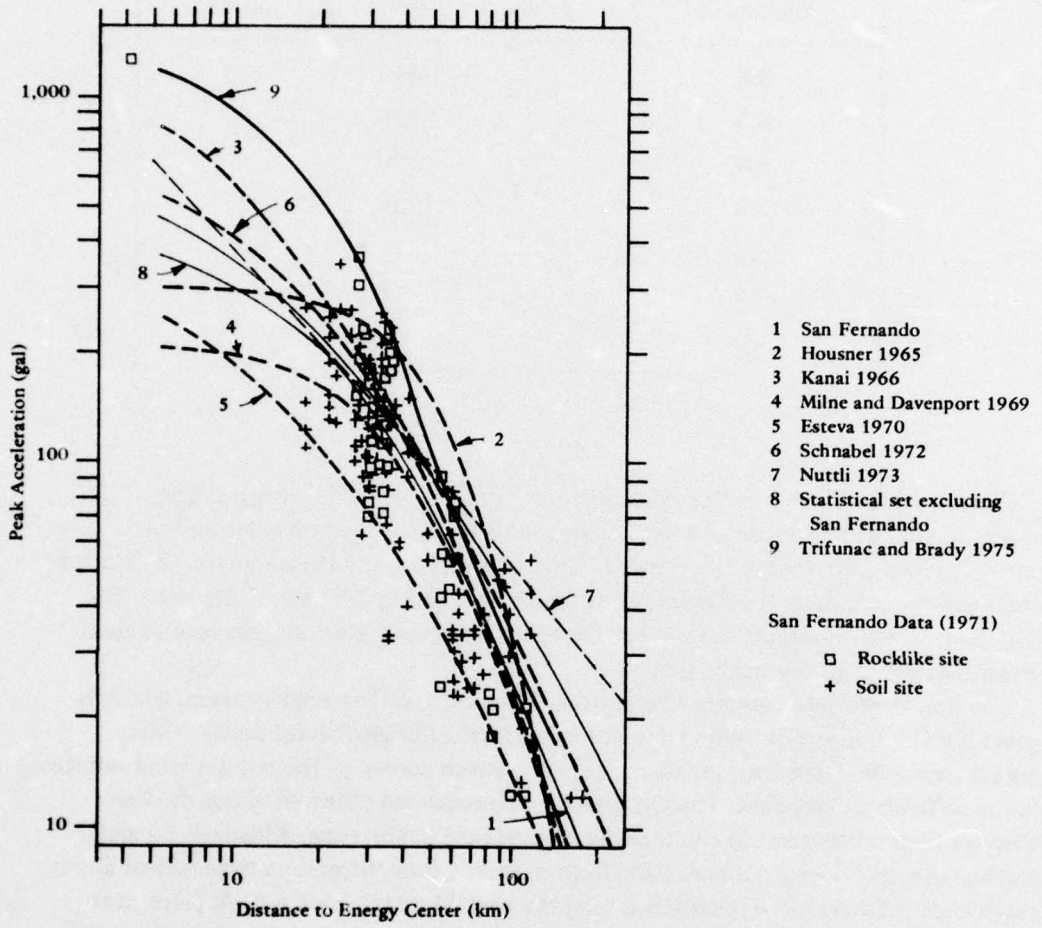

Figure 9. Attenuation equations for magnitude 6.5 earthquake compared to data recorded at strong motion stations during the San Fernando earthquake of February 1971.

Table 3. Magnitude Versus Length of Slipped Fault [20].

Magnitude	Length of Slipped Fault (miles)
8.8	1,000
8.5	530
8.0	190
7.0	25
6.0	5
5.0	2.1
4.0	0.83

Distant faults which must be considered of significance to the North Island region include the Elsinore and San Jacinto fault zones to the northeast and the San Clemente fault zone to the west. Local faults include the Rose Canyon, La Nacion, and Sweetwater faults, the Torrey Pines fault zone, and the Serrito Valley area. The San Andreas and Rampart fault zones are not considered significant because of their great distance from the study area.

The San Diego Bay contains Cretaceous, Tertiary, and Quaternary strata, which is generally flat but locally folded and cut by normal and right lateral faults. This area is called the Rose Canyon zone [21]. A bottom survey of the bay revealed numerous faults difficult to correlate. The Quaternary deformations observed along the Rose Canyon fault zone attest to the tectonic importance of the zone. Although no major earthquakes have occurred near San Diego in recent time, several earthquakes of about magnitude 3.5 have been recorded during the past 41 years. Eleven took place near the Rose Canyon fault. The magnitude 3.5 earthquake is associated with an 8 mm offset and a fault rupture length of 1 km. The geologic structure of this area shows evidence of previous movement. Surface traces of more than 15 miles in length and vertical separation of hundreds of feet are visible.

Table 4 shows the distance of key faults from the center of North Island, and the maximum credible earthquake and engineering-design-level earthquake determined from the length of the fault and its past history.

The following is a brief background on faults considered pertinent to this study [21 through 26].

Table 4. Fault Systems of Interest to NAS North Island[a]

Fault	Maximum Credible Magnitude	Design-Level Magnitude	Distance to Site (miles)	Length (miles)	Age
Elsinore	7.6	6.9 - 7.3	47	160	Historic
San Jacinto	7.6	6.9 - 7.3	67	180	Historic
San Clemente	7.7	–	50	110	Historic
Rose Canyon	7.1	6.5	2	–	Late Quaternary
La Nacion	6.8	–	8	15	Late Quaternary
Sweetwater	–	–	7	–	
South San Andreas	7.5	–	95	500+	Historic
Lyons Valley	–	–	20	–	–
Superstition Mountain	7	–	85	–	Historic
Engineer	–	–	23	–	–
Torrey Pines	–	–	–	–	Eocene
Sorrento Valley	–	–	–	–	Eocene
Morena	–	–	6	–	Eocene
Old Town	–	–	3	–	Eocene
Imperial	7	–	100	–	Historic
Tijuana San Miguel	–	–	55	–	–

[a]Blanks indicate unknowns.

the magnitude range of 3.5 to 3.7 were felt in the vicinity of San Diego Bay. Uplift has been noted near the fault in La Jolla in sediments that overlie the Linda Vista formation and are considered to be late Pleistocene (1,000,000 years old).

La Nacion Fault. This fault extends for 15 miles southward from La Mesa. The fault dips 60 to 70 degrees toward the west and consists of two or more branches; several are tens of feet apart. Offsets of Holocene deposits along the fault have been noted but not confirmed. There is definite evidence that Linda Vista formations (500,000 years) have been displaced. Evidence [23] suggests a change in the history of the San Diego Area, previously thought to be stable. Test borings approximately 30 meters deep show open faults in sedimentary rock, suggesting the area is in tension. Reference 23 notes that 1-km north of the Otay Valley the La Nacion fault offsets Pliocene formations, late Pleistocene terrace deposits, and Holocene alluvium (dating 10,980 ± 190 years).

Sweetwater Fault. The Sweetwater fault parallels the La Nacion fault for at least 15 km. The fault offsets late Pleistocene terrace deposits. This fault may continue into the Old Town fault.

Old Town Fault. Old Town fault consists of two main branches extending just to the east of San Diego Bay. Vertical offsets of late Pleistocene terrace deposits are easily seen.

Morena Fault. Morena fault is near the southern end of the Rose Canyon fault. The Morena fault trends across the Rose Canyon fault along the southern side of Mt. Soledad, crossing the inferred path of the Rose Canyon fault.

Earthquake-Induced Ground-Motion Levels

If the estimated magnitude of a seismic event and its distance from the site of interest are known, ground motion can then be predicted.

In order to understand the response of any point on the surface, determination of the surface topography and the underlying rock configurations are necessary. Types and characteristics of the soils determine soil response under dynamic loading. It is important to understand bedrock motion underlying the soil deposits and the transfer mechanisms to the surface. For earthquake engineering, bedrock may be defined loosely as a material exhibiting a seismic wave velocity of 2,500 ft/sec [16]. Peak rock outcrop acceleration is related to the distance from the fault rupture [24] (Figure 10). Empirical data on the relationship between rock accelerations, earthquake magnitude, and fault distance are scanty—especially for accelerations greater than 0.2 g—because few strong motion records have been obtained within 20 miles of a causative fault of magnitude 6 or greater.

San Jacinto Fault. The San Jacinto fault system extends from its junction with the San Andreas fault southeast of Palmdale to the Colorado River delta. Geodetic data indicate an average slip rate of 0.3 cm/yr. Seventeen large earthquakes have occurred since 1890 along the 180-mile-long fault. Those whose magnitudes were determined were in the range of 5.7 to 7.1.

This is one of the most active faults. In the 33-year period from 1890 to 1923, the northern portion of this fault system averaged an event each 5.5 years. Large earthquake activity in the northern half of the fault system has lapsed during the past 52 years. Movement in faults in the Imperial Valley caused an earthquake in 1915 and again in 1940 (25-year span). The last event was 35 years ago, and it is thought that significant strain has not been released since that event.

Whittier-Elsinore Fault. This fault system is composed of the Elsinore and Whittier fault zones, Agua Caliente fault, and Earthquake Valley fault. Five recent earthquakes of unknown magnitudes have occurred on this fault, the last one in 1935. No historical data exist to construct a recurrence relationship. A slip rate of 0.08 cm/yr was determined and used to calculate a recurrence interval. It is believed that sufficient elastic strain to produce a magnitude 6 or greater earthquake has accumulated along the fault in recorded historic time (several hundred years).

San Clemente Fault. This fault, with a verified length of 110 statute miles, extends from the eastern side of San Clemente Island to the Cabo Colonet area of Baja California, Mexico. A magnitude 5.9 earthquake occurred off the southeast tip of San Clemente Island in 1951. The maximum credible event for a fault of this length is 7.7 on the Richter scale. A significant consequence of an earthquake on this fault is the possible production of a tsunami or seismic sea wave, but such is not likely with magnitudes less than 6.3. Seven percent of southern California earthquakes have submarine epicenters, yet only two or three locally generated tsunamis are known to have occurred since 1800; none in the San Diego area.

Rose Canyon Fault. The Rose Canyon fault zone forms a belt of fractures about a mile wide. The zone on shore can be traced southwestward for a distance of more than 10 miles and then projects under San Diego Bay and continues to the Mexican border and possibly beyond (see Figure 8). An investigation of the bay [22] revealed many faults. North of La Jolla an offshore extension of the fault exists, suggesting that Rose Canyon is part of a much larger northwest trending zone of deformation that extends at least 150 miles from Santa Monica to Baja California and includes the Newport-Inglewood zone.* Geologic evidence suggests that the most recent movement was less than 500,000 years ago. Fault displacements as recently as early Holocene time (10,000 years ago) cannot be precluded; Reference 22 cites evidence of faulting through Pleistocene deposits. No large earthquakes have been associated with the Rose Canyon fault during historic time. During 1964, however, three earthquakes in

* Possible locus of the 1933 Long Beach earthquake, magnitude 6.3.

the magnitude range of 3.5 to 3.7 were felt in the vicinity of San Diego Bay. Uplift has been noted near the fault in La Jolla in sediments that overlie the Linda Vista formation and are considered to be late Pleistocene (1,000,000 years old).

La Nacion Fault. This fault extends for 15 miles southward from La Mesa. The fault dips 60 to 70 degrees toward the west and consists of two or more branches; several are tens of feet apart. Offsets of Holocene deposits along the fault have been noted but not confirmed. There is definite evidence that Linda Vista formations (500,000 years) have been displaced. Evidence [23] suggests a change in the history of the San Diego Area, previously thought to be stable. Test borings approximately 30 meters deep show open faults in sedimentary rock, suggesting the area is in tension. Reference 23 notes that 1-km north of the Otay Valley the La Nacion fault offsets Pliocene formations, late Pleistocene terrace deposits, and Holocene alluvium (dating 10,980 ± 190 years).

Sweetwater Fault. The Sweetwater fault parallels the La Nacion fault for at least 15 km. The fault offsets late Pleistocene terrace deposits. This fault may continue into the Old Town fault.

Old Town Fault. Old Town fault consists of two main branches extending just to the east of San Diego Bay. Vertical offsets of late Pleistocene terrace deposits are easily seen.

Morena Fault. Morena fault is near the southern end of the Rose Canyon fault. The Morena fault trends across the Rose Canyon fault along the southern side of Mt. Soledad, crossing the inferred path of the Rose Canyon fault.

Earthquake-Induced Ground-Motion Levels

If the estimated magnitude of a seismic event and its distance from the site of interest are known, ground motion can then be predicted.

In order to understand the response of any point on the surface, determination of the surface topography and the underlying rock configurations are necessary. Types and characteristics of the soils determine soil response under dynamic loading. It is important to understand bedrock motion underlying the soil deposits and the transfer mechanisms to the surface. For earthquake engineering, bedrock may be defined loosely as a material exhibiting a seismic wave velocity of 2,500 ft/sec [16]. Peak rock outcrop acceleration is related to the distance from the fault rupture [24] (Figure 10). Empirical data on the relationship between rock accelerations, earthquake magnitude, and fault distance are scanty—especially for accelerations greater than 0.2 g—because few strong motion records have been obtained within 20 miles of a causative fault of magnitude 6 or greater.

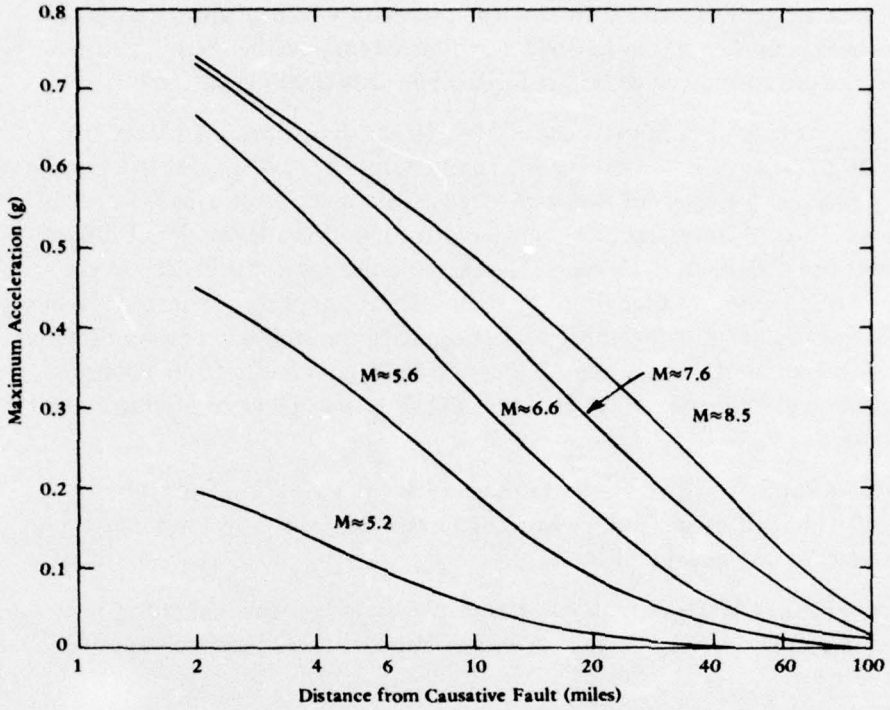

Figure 10. Average values of maximum accelerations in rock.

Figure 11, a map summary of a study by Greensfelder [25], shows contours of possible peak acceleration from active faults in southern California. The probability of occurrence is not considered, other than that the faults believed to be active include Quaternary movement. The North Island area is noted to be capable of peak accelerations of 0.5 g.

For California earthquakes the focal depth is typically 10 to 15 km, which is comparatively shallow. In general, this type of earthquake produces higher accelerations at the ground surface for points located near the fault and epicentral region. Amplitudes of acceleration decrease with distance from the fault, and the predominant period increases with distance.

Data on the predominant periods of rock acceleration show a large amount of scatter. Figure 12 [20] gives predominant periods as a function of distance. Table 5 [19, 25] gives the duration of shaking. These are subjective estimates rather than precise calculations. Duration of shaking is influenced by earthquake magnitude because shaking is likely to continue at least as long as rupture propagates along the fault.

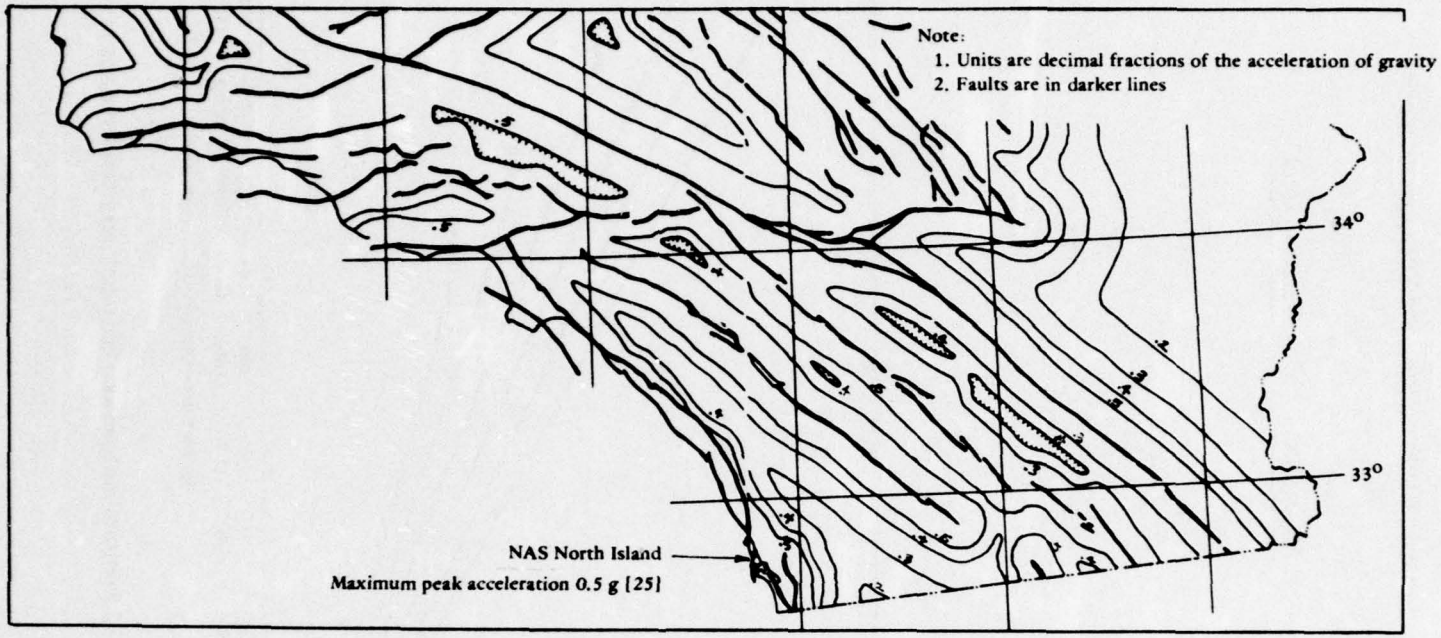

Figure 11. Maximum credible rock accelerations.

Table 5. Richter Magnitude Versus Earthquake Duration

Magnitude	Duration (sec)
5	5
6	15
6.5	18
7	25
7.5	30

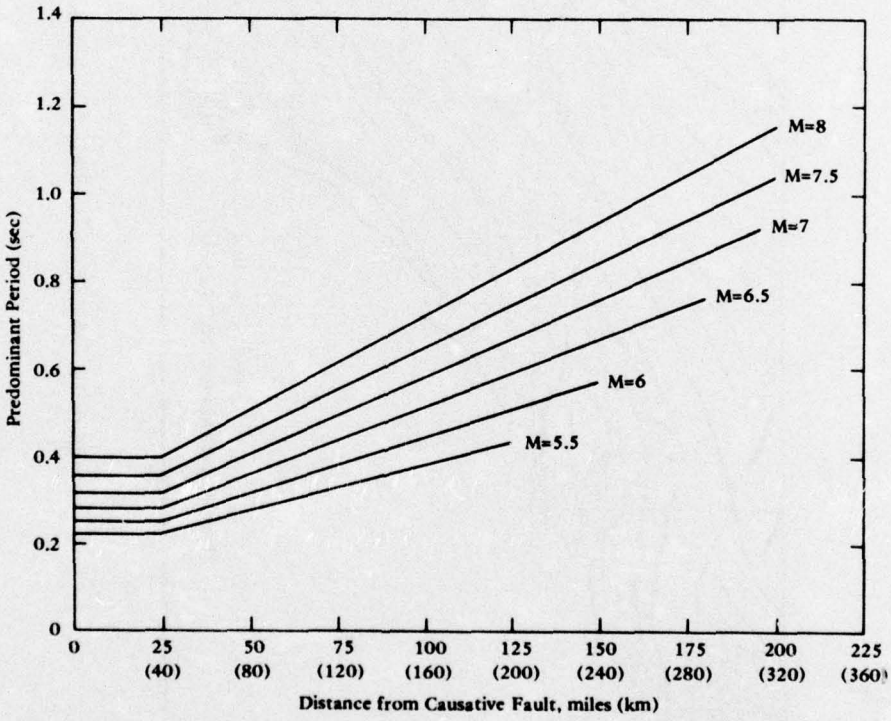

Figure 12. Predominant periods for maximum accelerations in rock.

The rate of rupture is believed to be on the order of magnitude of 2 miles/sec [20], so that a magnitude 7 earthquake resulting from a 25-mile fault would have a duration of at least 12.5 seconds.

An acceleration time history for use in seismic design studies can be generated with desired characteristics by use of random number programs or obtained by modifying existing earthquake records. For best results, a record having the desired predominant period should be scaled.

Probability of Occurrence

Occurrence data have been developed for the Elsinore and San Jacinto faults (Figure 13) based on historic data [21]. Since these are very active faults, historic data is available; the large number of occurrences makes this approach valid. However, for the Rose Canyon fault, which does not exhibit much activity, this approach is not possible. In Reference 22 recurrence data were developed for the San Diego area based on the rate of slip. This approach followed the work reported in Reference 18; recurrence data shown in Figure 13 for Rose Canyon is based on this. Note the activity of the Rose Canyon fault is an order of magnitude less than that of the other two faults. Table 6 [26] gives historical earthquakes with epicenters in the North Island area since 1932. The 42 earthquakes demonstrate that slip is in progress in the area. A recurrence curve based on this limited data is also shown in Figure 13, but the absence of any large events biases the data. Note that the slope of the historical curve for magnitudes around 2.5 (where many data points exist) is the same as that of Reference 22. This indicates the potential for a significant earthquake in the area. Probability-of-occurrence curves, based upon the foregoing, were computed, assuming a Poisson distribution (see Figures 14, 15, and 16). For design purposes, NAVFAC criteria specify use of an earthquake magnitude with 10% chance of being exceeded in 25 years.

EARTHQUAKE RESPONSE AND LIQUEFACTION ANALYSIS

General Discussion

Before an analysis of liquefaction potential can be made it is necessary to have an estimate of the ground motions and dynamic shear stress loading of the soil. One approach is to estimate the peak bedrock motion, develop a suitable earthquake bedrock time history, and compute the surface motions and soil stress histories at the depths of interest.

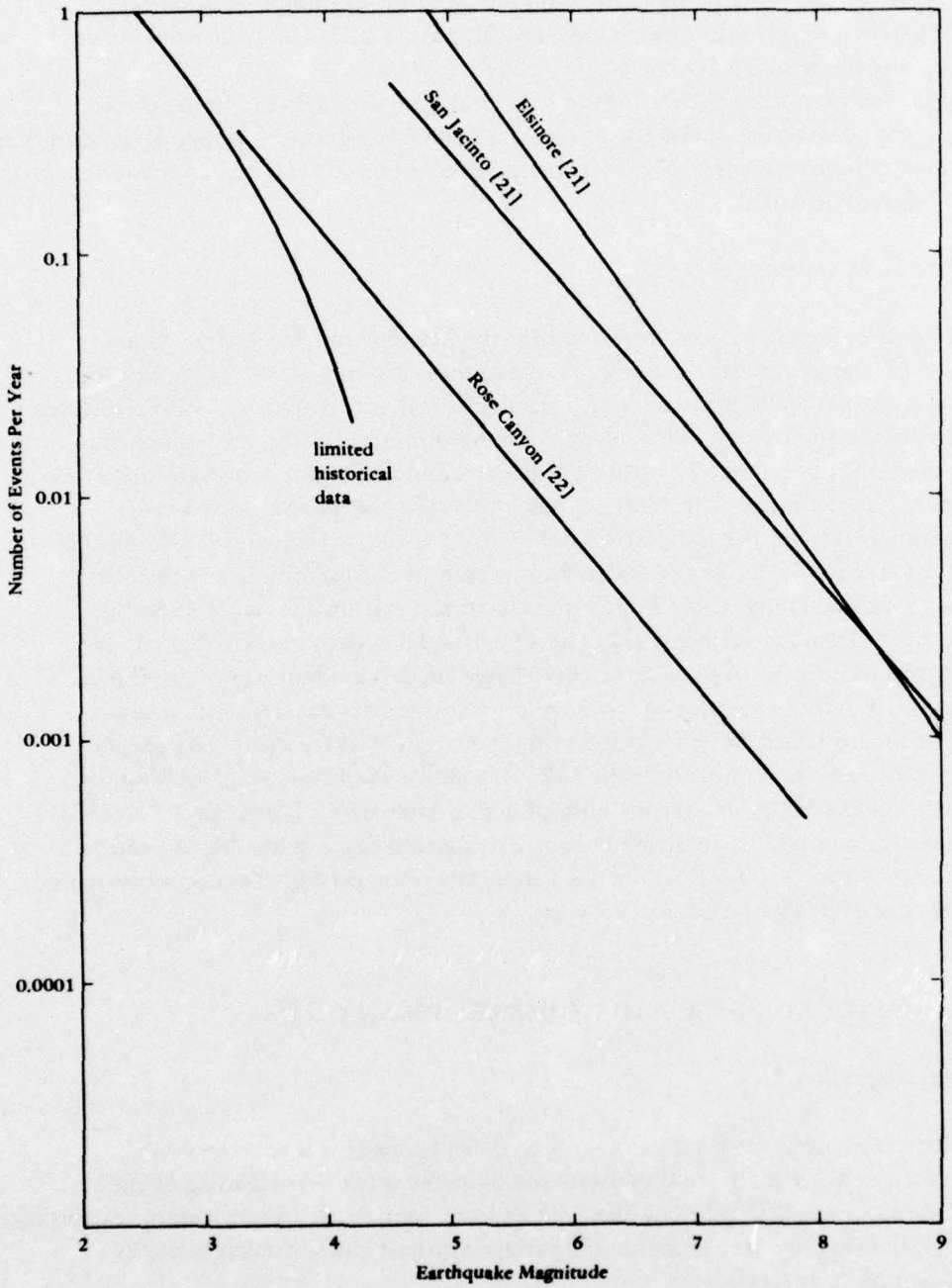

Figure 13. Recurrence data for three faults.

Table 6. Earthquakes Experienced in the San Diego Area Between 1934 and 1972

Year	Latitude (N)	Longitude (W)	Magnitude
1934	32 53 0 32 58	117 30 0 117 22 8	2.5 3.5
1936	32 50 32 50	117 30 117 30	3 2.5
1938	32 42	117 24	2.5
1939	32 30	117 15	2.5
1940	32 54	117 30	2.5
1941	32 53	117 24	3.0
1943	32 51	117 29	4
1946	32 43	117 25	3.3
1948	32 48 32 30	117 12 117 5	2.5 3.0
1949	32 55 32 48 32 33 32 52 32 43 32 51 32 52 32 52 32 59	117 18 117 20 117 16 117 20 117 21 117 0 117 15 117 15 117 16	3.0 2.9 2.8 3.1 2.5 2.3 2.4 2.4 2.3
1958	32 34	117 9	3.7
1960	32 49	117 3	2.5

continued

Table 6. Continued

Year	Latitude (N)	Longitude (W)	Magnitude
1961	32 49 32 40	117 5 117 3	2.7 3
1962	32 38 3 32 48 6	117 18 4 117 7 9	3.2 2.9
1963	32 55 32 35 4 32 45 3	117 30 117 18 3 117 8 8	2.9 4.2 2.6
1964	32 49 2 32 41 5 32 42 3 32 41 4 32 47 8	117 3 5 117 9 7 117 6 8 117 7 4 117 8 2	2.8 2.7 3.5 3.6 2.8
1965	32 55 0	117 34 6	3.1
1966	32 53 1	117 11 4	3.2
1968	32 49 32 41 1	117 3 3 117 5 7	2.9 3.5
1970	32 47 9	117 4 9	2.5
1971	32 31 1	117 4 6	3.3
1972	32 57 9	117 37 2	3.2

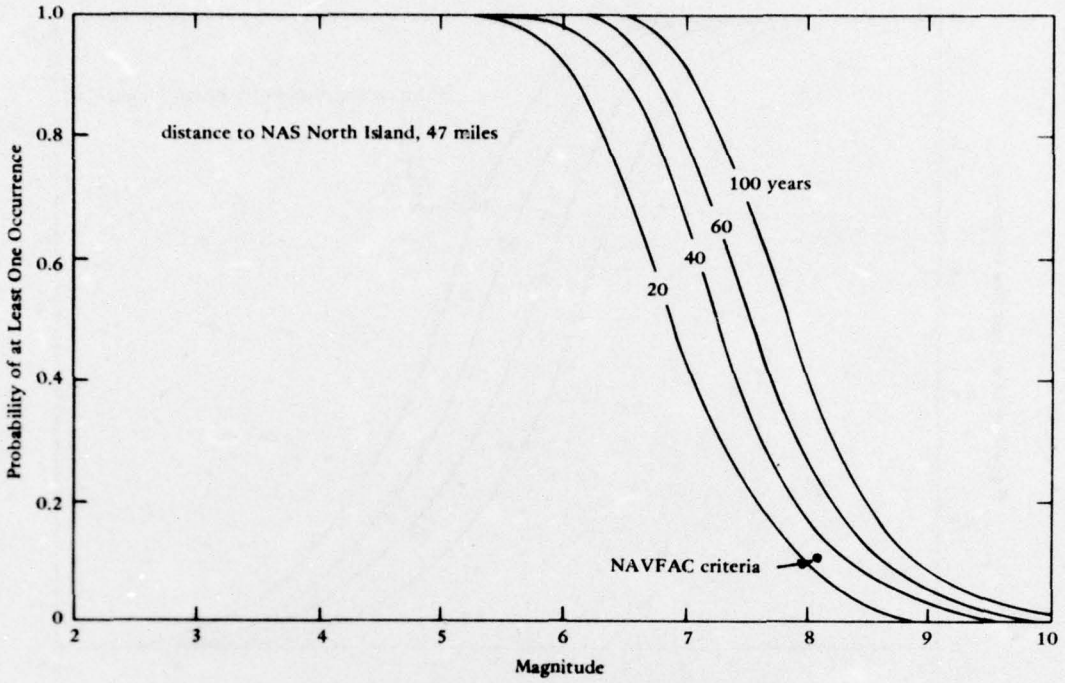

Figure 14. Probability of earthquake occurrence on the Elsinore fault.

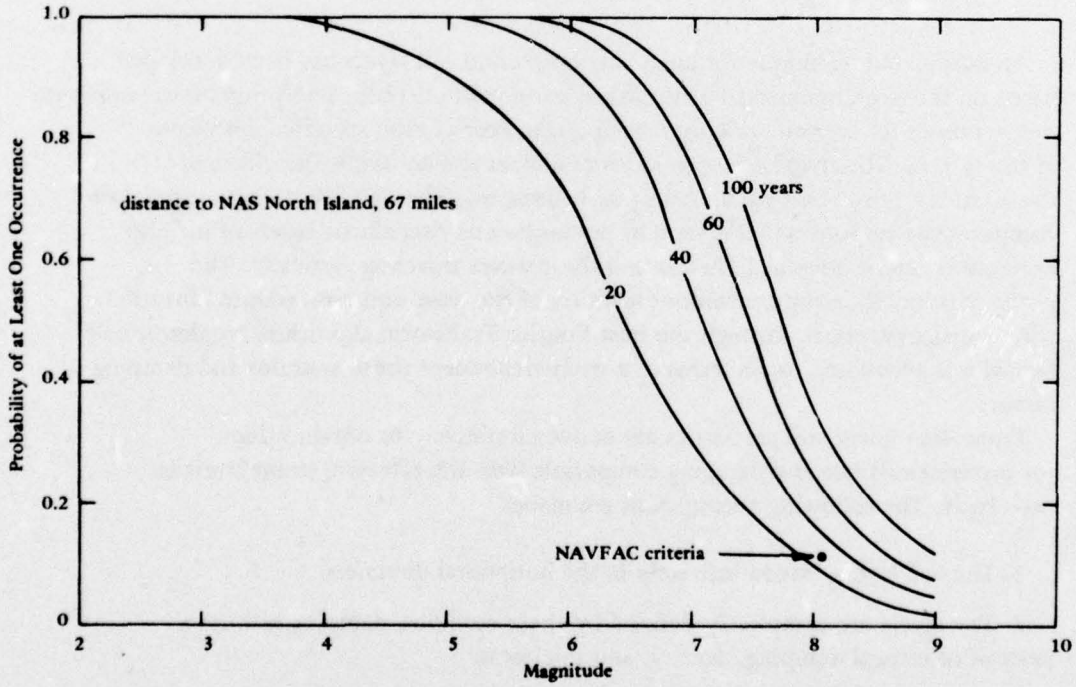

Figure 15. Probability of earthquake occurrence on the San Jacinto fault.

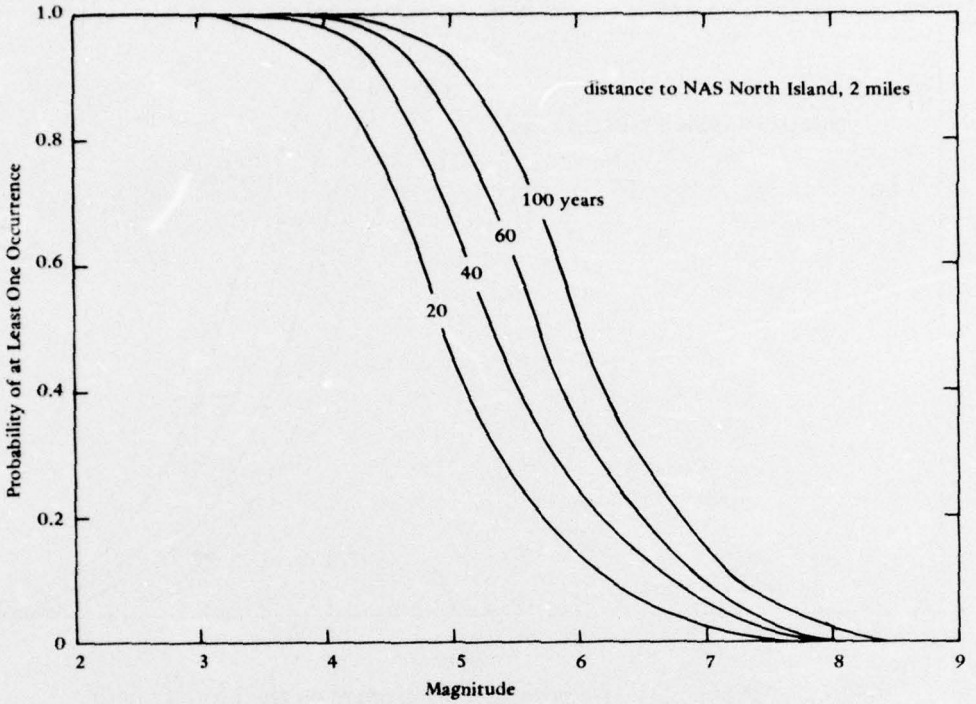

Figure 16. Probability of earthquake occurrence on the Rose Canyon fault.

An automated technique for analyzing horizontal soil layers has been developed, based on the one-dimensional wave-propagation method [27]. This program can compute the responses for a given horizontal earthquake acceleration specified anywhere in the system. The analysis incorporates nonlinear soil behavior, the effect of the elasticity of the base rock, and variable damping. The SHAKE computer program computes the responses in a system of homogeneous viscoelastic layers of infinite horizontal extent, subject to horizontal shear waves traveling vertically. The program is based on the continuous solution of the wave equation adapted for use with transient motions through the Fast Fourier Transform algorithm. Nonlinear soil behavior is accounted for in terms of a strain-dependent shear modulus and damping factor.

Equivalent linear soil properties are derived iteratively to obtain values for material stiffness and damping compatible with the effective strain levels in each layer. The following assumptions are made:

1. The soil layers extend infinitely in the horizontal direction.

2. The layers are completely defined by shear modulus, damping ratio as a percent of critical damping, density, and thickness.

3. The soil values are independent of frequency.

4. Only vertically propagating, horizontal shear waves are considered.

The soil model has properties similar to those developed by Hardin and Drnevich [28, 29]. Specification of soil response is facilitated by incorporation of a variable coefficient, which automatically provides for modification of soil parameters with effective strain. Different relationships are included for sand, clay, and rock. The program will use this data unless the programmer replaces it with his own specific relationships. The modulus of sand is made a direct function of either the square or cube root of confining stress. The absolute range of soil parameter variation may be stipulated by merely putting in factors whose numerical values may be derived from simple soil strength properties. These strength properties may be the undrained shear strength of a clay or the relative density of a sand, defined as:

$$D_r = \frac{e_{max} - e}{e_{max} - e_{min}} = \frac{\gamma_{max}}{\gamma} \frac{(\gamma - \gamma_{min})}{(\gamma_{max} - \gamma_{min})}$$

where D_r = relative density

e_{max}, γ_{min} = maximum void ratio and minimum dry density, respectively (soil in its densest possible state)

e_{min}, γ_{max} = minimum void ratio and maximum dry density, respectively (soil in its densest possible state)

e, γ = void ratio and dry density, respectively, of a soil in its natural state

This program will use input values of soil modulus (or derive it from input shear wave velocity) and damping ratio for its first iteration, but thereafter will pursue a compatibility between calculated strains and the various incorporated material response models.

More involved methods of analysis are available, particularly those based upon finite element analysis [30, 31]. These latter methods are desirable for complex soil profiles or where soil structural interaction must be considered.

For liquefaction in a specific soil profile the stress history of the various layers must be compared to their susceptibility to liquefaction. The liquefaction susceptibility under earthquakes may be measured directly under cyclic loading [32] or estimated on the basis of a critical void ratio, dependent upon applied dynamic stress levels [33]. Since the former method is best defined and most validated to date, at least with respect to earthquake loads, it will be the only one discussed here. The stress history to which a specific soil stratum is subjected during an earthquake must first be determined analytically.

For the direct cyclic load testing approach, the history of the calculated shear stress due to the earthquake is equated to a specific number of shear stress cycles of a particular amplitude [32, 34]. Soil specimens are then prepared and subjected to cycles of shear stress necessary to cause liquefaction. The two test approaches most commonly used are based upon reversed loading triaxial testing [35] and simple shear testing [36, 37]. Additional testing techniques exist, such as those based upon torsional shear of hollow cylinders [38], but this equipment is not widely available and will not be discussed further. Unfortunately, laboratory testing does not generally simulate actual field conditions; therefore, correction factors are commonly required for correlation with in-situ earthquake response [39].

Soil test data is commonly presented in terms of the number of uniform, or symmetrical, cycles of shear stress at a particular stress level required to cause liquefaction of material under specific conditions of density and static confining stress. Previous work [40] suggests that the number of cycles necessary to cause liquefaction of any granular material is a direct function of the dimensionless ratio:

$$\frac{\tau}{\sigma_c D_r}$$

where τ = the alternating dynamic shear stress level

σ_c = represents the static effective confining stress level

D_r = is the relative density of the soil, defined previously

For the triaxial test the value of τ is taken as one-half the maximum deviator stress application, which is the maximum shear stress to which the speciman is subjected. The confining stress is taken as σ_3, the chamber pressure. For the simple shear test τ is the dynamic shear stress applied to the horizontal plane, whereas the confining pressure is taken as the vertical stress.

Data compiled from triaxal test results (see Figure 17) has been combined with stochastic methods to provide a simplified computer program for prediction of liquefaction [40]. The earthquake record is represented in terms of the peak acceleration and duration and a predominant frequency. The program determines the stress history at specific locations based upon Newton's law. Application of Minor's Linear Damage Criterion, together with the relationship shown in Figure 17, permits determination of a factor of safety against liquefaction.

Liquefaction at NAS North Island

The earthquake magnitude and ground motion levels based on the NAVFAC design criteria applied to the recurrence curves of Figures 14, 15 and 16 are summarized in Table 7.

Table 7. NAVFAC Design-Level Earthquakes at North Island

Fault Name	Magnitude of Design Earthquake (Richter Scale)	Distance from NAS North Island (miles)	Predicted Peak Rocking Motion (g)
San Jacinto	8.1	67	0.09
Elsinore	8.1	47	0.15
Rose Canyon	6.4	2	0.60

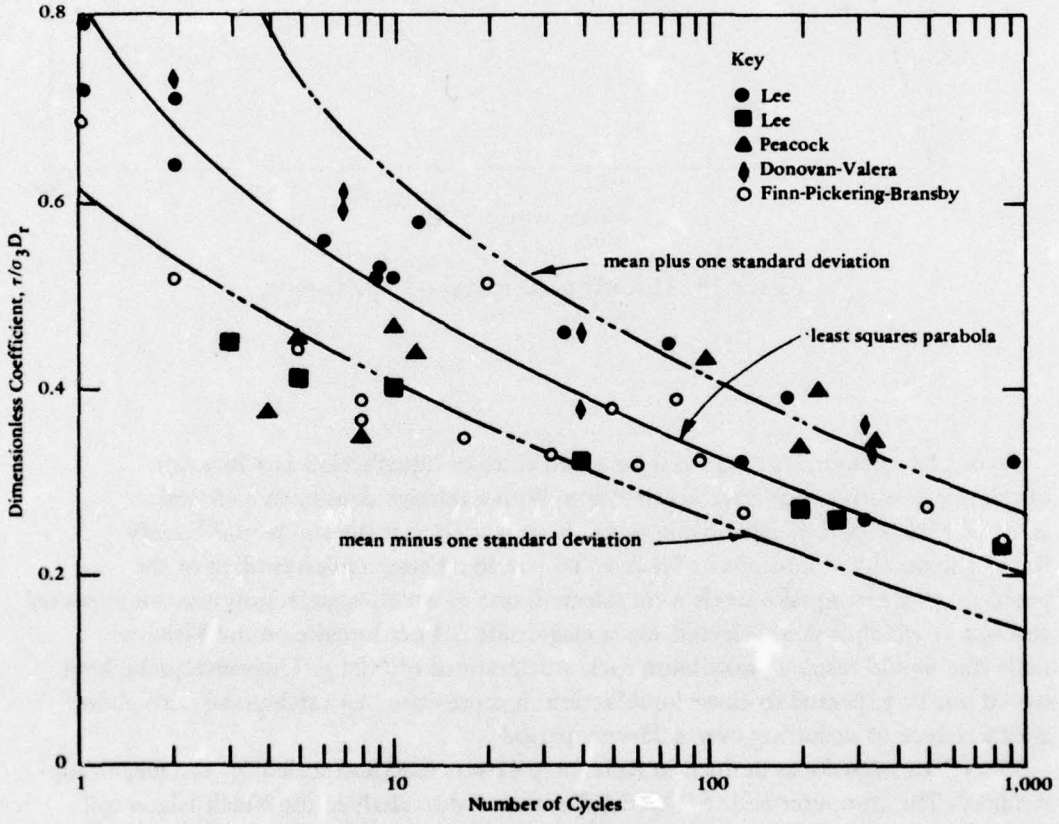

Figure 17. Stress ratio for liquefaction.

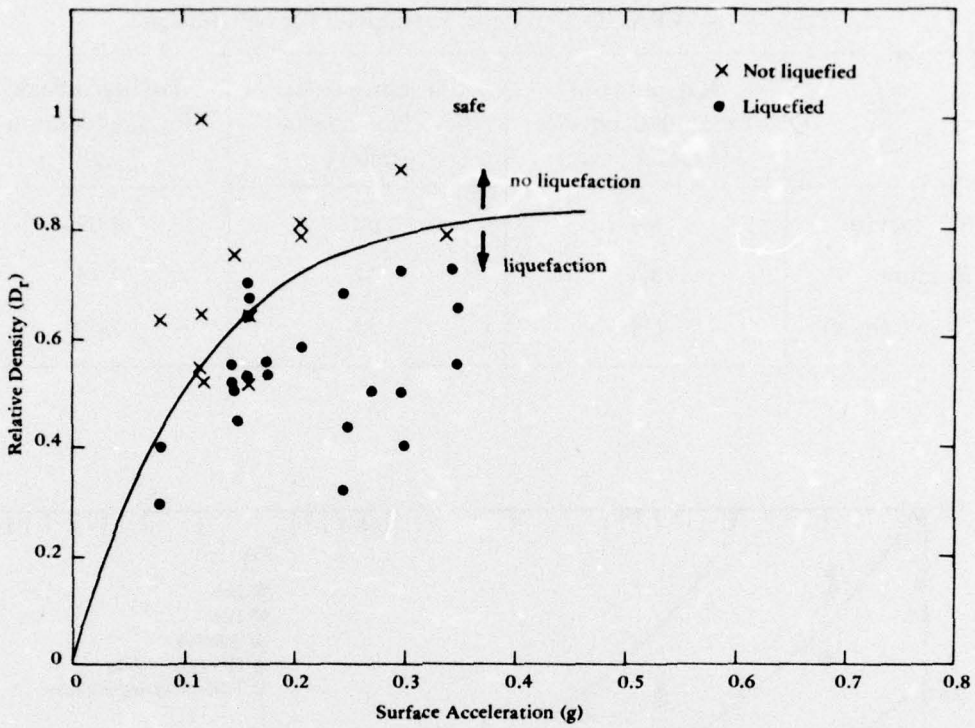

Figure 18. Historic occurrences of liquefaction.

Figure 18 summarizes data from observed cases of liquefaction as a function of relative density and surface acceleration. With a relative density in a critical layer of 35% (Figure 6, layer 5), it would be expected that the soil would liquefy for all the predicted motions in Table 7. To obtain a better understanding of the problem, two earthquake levels were selected; one at which liquefaction was not expected and one at which it was. Selected was a magnitude 6.4 earthquake on the Elsinore fault that would result in maximum rock accelerations of 0.04 g. This earthquake level would not be expected to cause liquefaction; it represented an earthquake with about a 90% chance of occurring over a 25-year period.

The C1 earthquake as defined in Reference 41 was used and scaled for the magnitude required. The computer code SHAKE [27] was used to analyze the North Island soil profile shown in Figure 6. Figure 19 is a plot of maximum acceleration generated versus depth. Also shown on the figure is a simplified soil profile for easy reference.

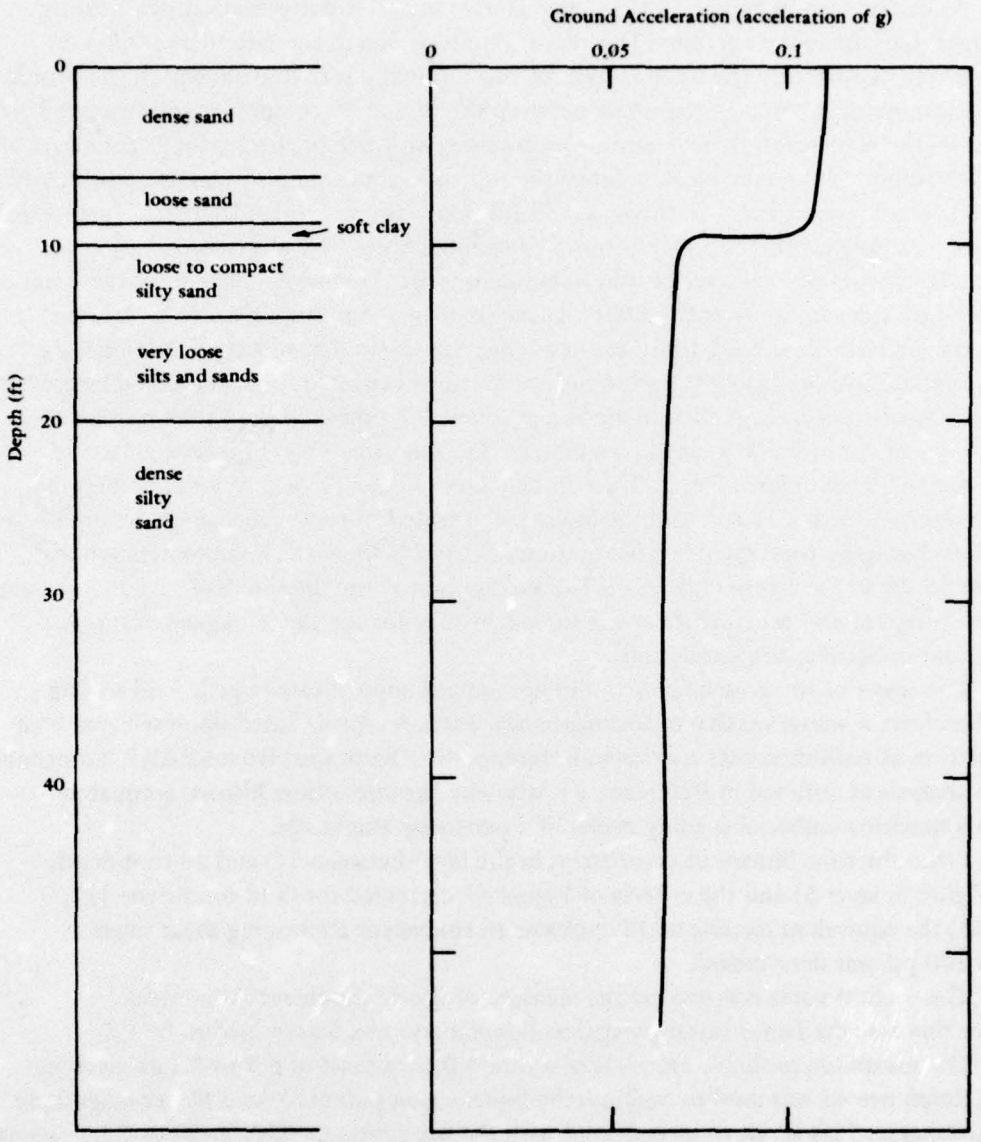

Figure 19. Soil accelerations for a magnitude 6.4 earthquake on the Elsinore fault.

As can be seen in Figure 19 the upper 10 feet of soil sustains motion significantly larger than the lower portions. This discontinuity is due to the 1-foot layer of very soft clay. Apparently the introduction of this unusually soft stratum within the profile has resulted in a complex harmonic between the two more competent soil zones (above and below the soft stratum). The harmonic coincides with one of the predominant harmonics of the input earthquake motion. Since the soil zone above the soft clay is not of interest to the liquefaction analysis, this interrelationship was not explored further. Furthermore, it is not known if this soft clay forms a continuous layer over a very broad area, or if it consists of a number of thin noninterconnected segments. Obviously the latter case would react significantly different from that of a continuous strata, as assumed in the analysis. Figure 20, based on Reference 42, shows that in a typical soil having acceleration values below 0.1 g the surface motions expected for a soil would be greater than those for a rock. A surface motion of about 1.7 times the peak rock motion of 0.04 g—or about 0.068 g—would be expected in this case. This is the level observed in the soil layer below 10 feet. The soft clay layer behaves as a very weak link (spring) between the upper 10 feet and the lower soil profile and results in significant amplifications. Damping coefficients varied between 3.3 and 8.4% in the cohesionless soil and was 15.2% in the 1-foot clay layer. The average period for the soil deposit was 2 seconds. The program also provides shear-stress/time history for the various layers of interest for use in liquefaction predictions.

The scope of the present project did not include sophisticated cyclic load testing. Therefore, it was necessary to formulate liquefaction criteria based upon selected compilation of published data such as in Reference 40. The output from SHAKE is amenable to analysis as outlined in Reference 34, whereby the stress/time history is equated to a specific number of loading cycles of a particular amplitude.

From the time history of shear stress in the layer between 15- and 20-foot depth (Figure 6, layer 5) and the criteria of Figure 17 corrected for field conditions [32, 39], the equivalent loading of 13 cycles at an equivalent alternating shear stress of 100 psf was determined.

The vertical stress was used as the measure of the confinement in the field. For this case the factor of safety against liquefaction was determined to be 1.5.

The maximum probable earthquake on the Elsinore fault of 6.9 to 7.3 as specified in Reference 43 was used to evaluate the liquefaction potential for a higher magnitude earthquake. This is not to be confused with the maximum credible event of 7.6 magnitude. The 6.9 to 7.3 event selected for analysis would have a 50% chance of being exceeded in 25 years, (and, therefore, is of a lower magnitude than that required by the NAVFAC criterion). It will be noted that the NAVFAC design-level earthquake of 8.1 (Table 7) exceeds that of the maximum credible event. This serves to illustrate shortcomings in predictions based upon limited recurrence data. The recurrence curves plotted in Figure 13 are based primarily upon small events. It is obvious that projecting them into the large-event range results in conclusions that are inconsistent with available

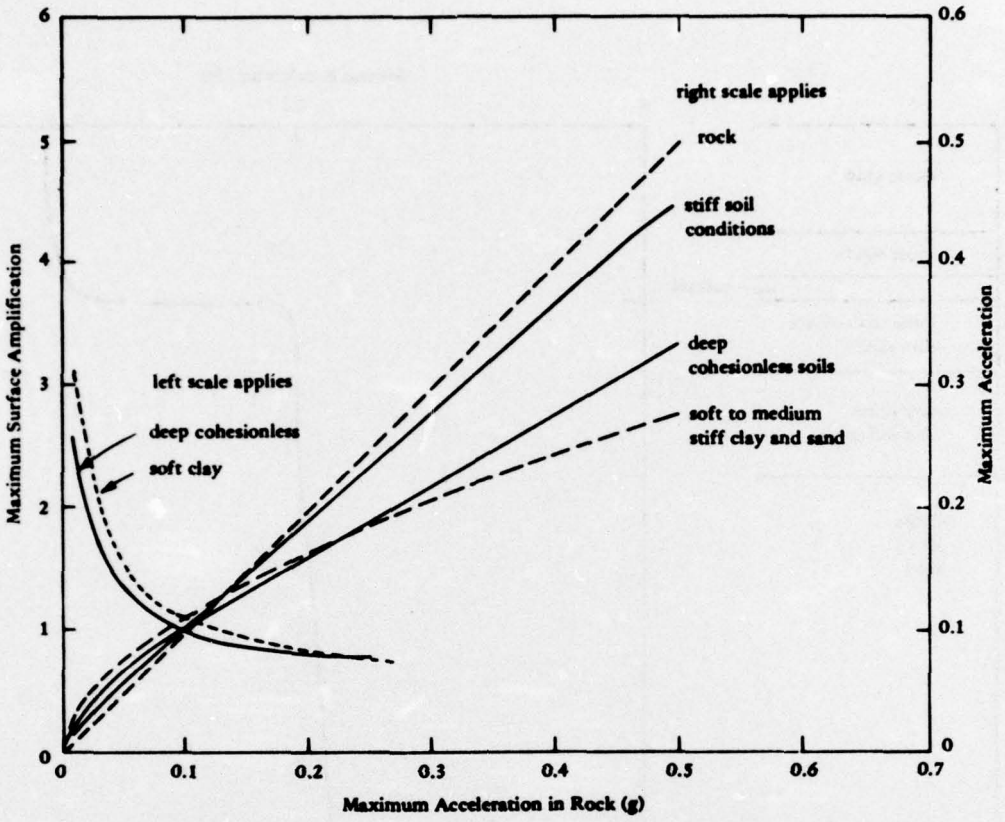

Figure 20. Approximate relationships between maximum accelerations for different soil conditions.

geologic data. Whether this inconsistency is due to incomplete geologic data or to the limited historical period of observation cannot be answered with certainty.

A magnitude 7.0 earthquake having rock outcrop motion of 0.07 g was selected and was expected to produce liquefaction. The analysis was repeated; ground accelerations versus depth are shown in Figure 21. The motion in the upper 10 feet of soil was again larger than the lower soil layers due to the soft clay layer. Figure 20 indicates the expected soil amplification would be about 1.35, providing for 0.07-g rock motion and about 0.095-g soil motion. This is about the level of motion observed below the 10-foot-depth level. Since the motion was at a higher level, the damping in the cohesionless layers was higher than in the previous case (4.5% versus 12.2%) and the damping in the clay layer was 20.2% of critical. Note also that the amplification ratio was decreased from the case of the 0.04 g acceleration level. In the manner explained previously, the number of equivalent cycles for the ground response was found to be about 25 cycles at an alternating shear stress level of 150 psf. The factor of safety was found to be 0.9, indicating that liquefaction would occur.

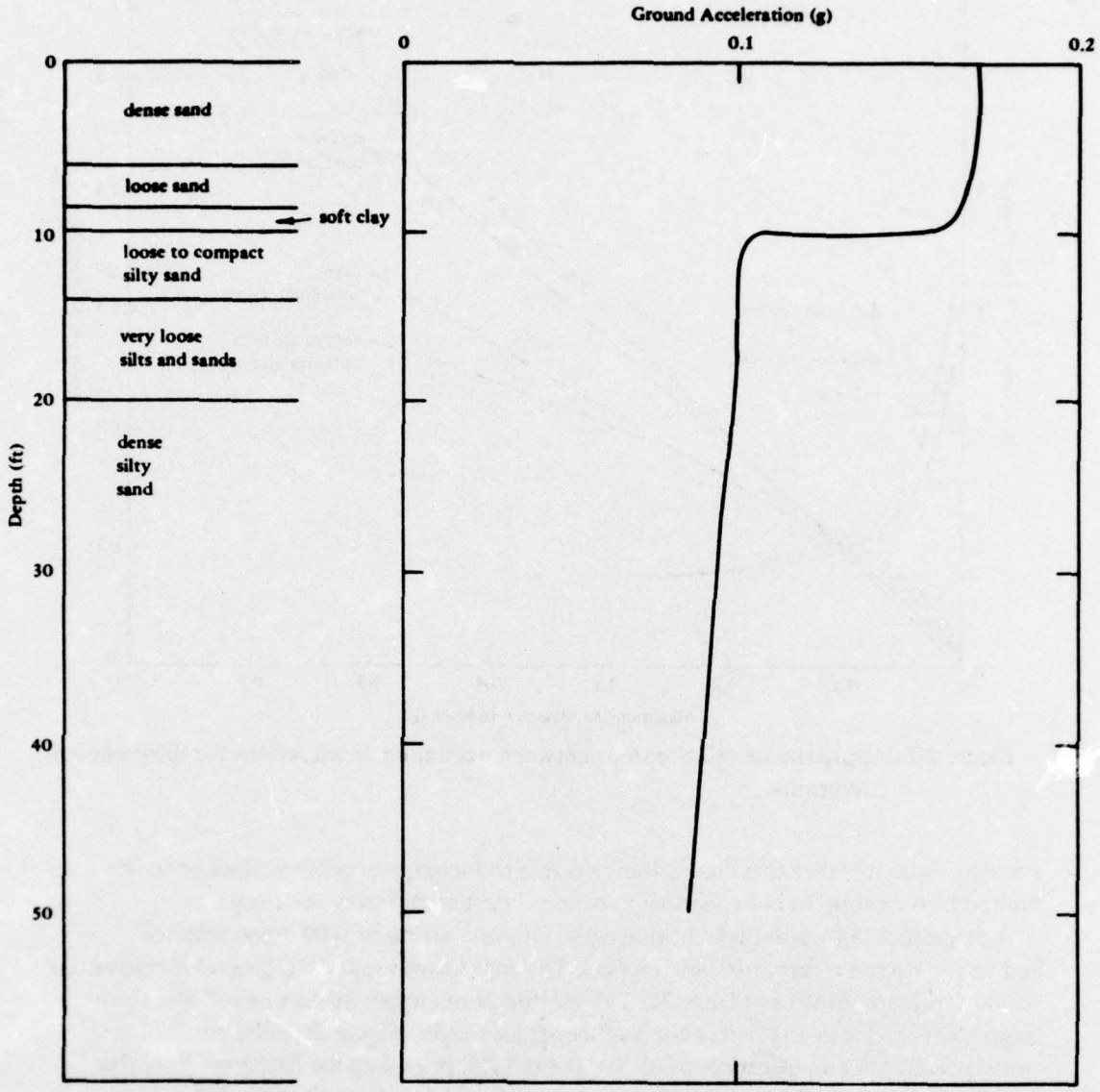

Figure 21. Soil accelerations for a magnitude 7.0 earthquake on the Elsinore fault.

Additionally, an analysis was performed using the liquefaction analysis code of Reference 40, and again an earthquake on the Elsinore fault was considered. The soil layer between the 15- and 20-foot depths, with an estimated relative density of 35%, was selected as the most likely candidate for liquefaction. Various earthquake levels were used to give the factor of safety versus earthquake magnitude relationship shown in Figure 22.

Liquefaction would be expected to occur at a magnitude about 6.9 on the Elsinore fault, which is a lower level of earthquake motion than would be stipulated by NAVFAC criteria. This would correspond to a surface site acceleration of 0.13 g. The results of this simplified analysis agree with the more detailed computer results obtained by SHAKE (see Figure 22). Considering the reliability of the input data, the simplified analysis was considered appropriate for the remainder of this work.

In Figure 23 the earthquake magnitude required to cause liquefaction at North Island is shown as a function of distance from the site. Also shown are known faults and the maximum credible and various design-level earthquakes. The NAVFAC criteria of selecting an earthquake with 10% chance of not being exceeded within a 25-year period results in high magnitude earthquakes such that liquefaction would be expected at North Island due to possible events on several faults. The selection of lower magnitude earthquakes, however, such as the maximum probable earthquake on the Elsinore fault would also result in liquefaction. Figure 23 can be used in conjunction with Figures 14, 15, and 16 to show the probability of an event for a given time span.

GROUND MOTION AND LIQUEFACTION POTENTIAL

Two major problem areas exist in carrying out a liquefaction analysis: (1) determining the ground motion to be expected from an earthquake and (2) determining the soil properties of the site, particularly the susceptibility to liquefaction.

The soil response parameters of direct interest to liquefaction may be divided into two major groups. The first group, such as soil modulus and damping ratios, defines the overall response of the soil profile to a specific earthquake stimulation. The second group—those parameters that control rate of pore water buildup, deformation rates, strength reduction under load, etc.—defines what happens to the soil while it is undergoing the specific motion. The two types of response parameters are directly interrelated under actual conditions but generally must be separated incrementally for analysis.

Earthquake Ground Motions

Determination of potential earthquake activity for engineering analysis is a study area requiring considerable judgment. The NAVFAC criteria suggest use of an earthquake magnitude with a 10% chance of being exceeded in 25 years. This magnitude must be based on the seismic activity associated with a given fault. The designation of a fault as active requires detailed geologic investigation for movement over geologic time. The

timespan used for designating a fault as active for earthquake analysis is somewhat questionable. Most of the larger events that have taken place in southern California have occurred on faults with no prior recorded activity. When a fault is historically active, the data is usually so very sparse that recurrence data may not be very reliable. Furthermore, a Poisson distribution may not be an accurate representation of the time distribution of earthquake occurrences.

Use of the NAVFAC criteria in the case of the Elsinore fault results in an earthquake magnitude of 8.1, greater than the maximum credible event of 7.6 suggested in Reference 43. Thus, the value of 8.1 probably is not valid, and the 7.6 magnitude should be a limiting value. For the case of the Rose Canyon fault the NAVFAC criteria indicate a 6.4 magnitude, and the design-level earthquake suggested in References 1, 16, and 22 is 6.5.

Although some success has been achieved in relating fault length to earthquake magnitude, prediction of rates of ground-motion attenuation based on distance is still a very inexact procedure (see Figure 9). In addition, the specific properties and characteristics of the site or the foundation conditions through which the ground motions must propagate are important but are rarely known with any certainty. Input ground motion to the liquefaction analyses may vary by 100%, using the best available techniques.

Detailed geologic investigation is required to determine the location of bedrock and the seismic velocities of the soil layers. This may be accomplished by seismic exploration, although other types of investigation may also be used, such as resistivity, borings, etc. Unfortunately, such expensive field investigations can only be justified in large projects. Moore and Kennedy, reporting in Reference 22 on the faults in the San Diego Bay area, show an extension of the Rose Canyon fault crossing North Island, but no detailed geologic study of this area has been performed.

Evaluation of In-Situ Conditions

The approach to site liquefaction analysis herein has evolved largely from the efforts of Professor H. B. Seed at the University of California at Berkeley [32, 35, 36, and 39] and permits use of the results of the Standard Penetration Test (SPT) [6, 8, 9, 44, 45]. The SPT is the most expedient and popular procedure used in North America for evaluating the in-situ properties of granular soils, particularly those below the water table. Although this form of foundation investigation has a long-established record for use in conventional foundation design, it is pointed out by various workers [46, 47, 48] that the SPT was never intended to provide numerical quantitative data such as that required for liquefaction analysis. Dynamic drive sampling, such as the SPT, is generally used in liquefaction analysis to provide numerical values of relative density, D_r, through use of blow-count/density correlations such as those of Reference 44 (also see Table 1). This value of D_r may then be used to reconstitute specimens for cyclic testing or may be used directly with relationships such as those of Figure 17 for liquefaction evaluations.

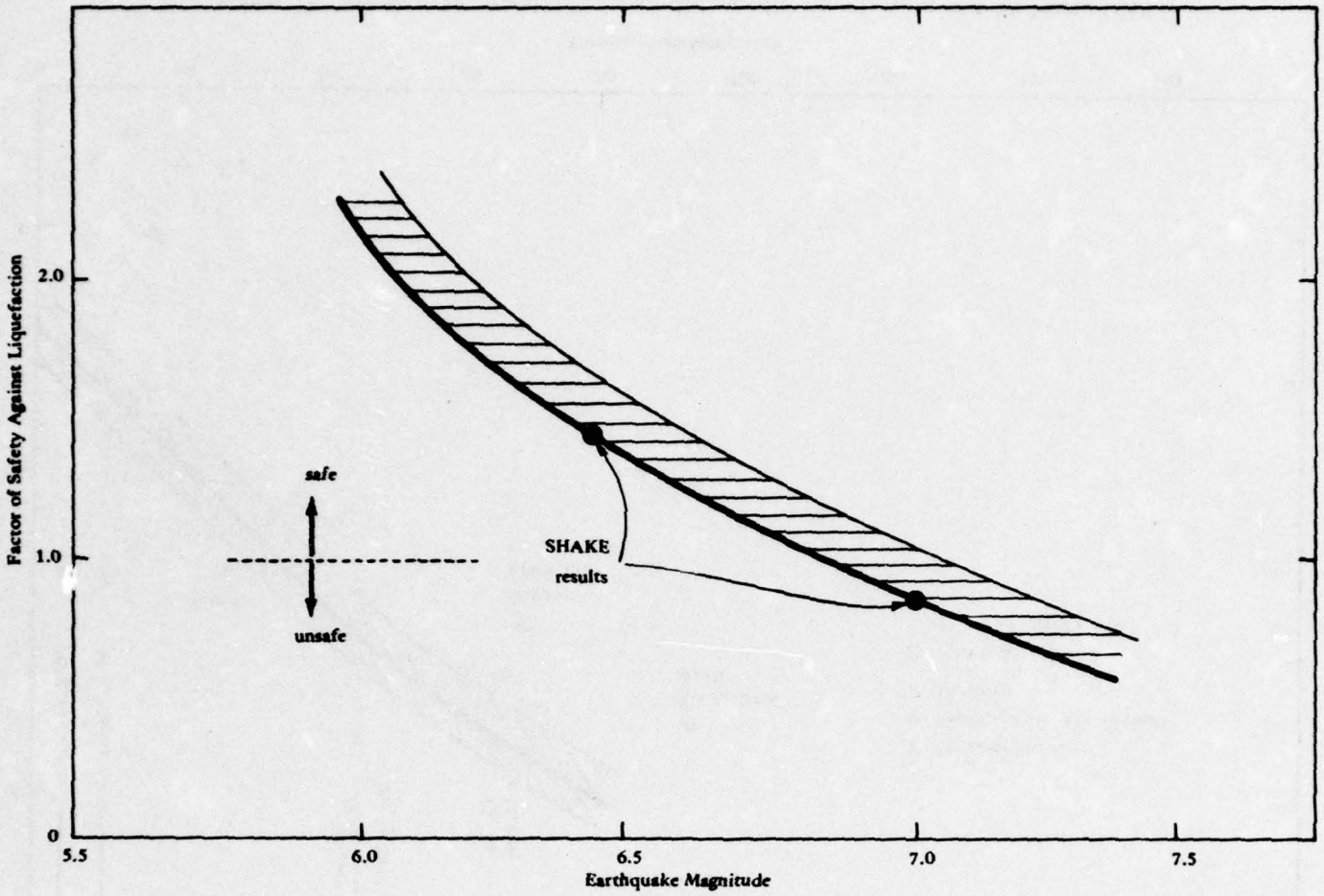

Figure 22. Factors of safety for different earthquake magnitudes on the Elsinore fault.

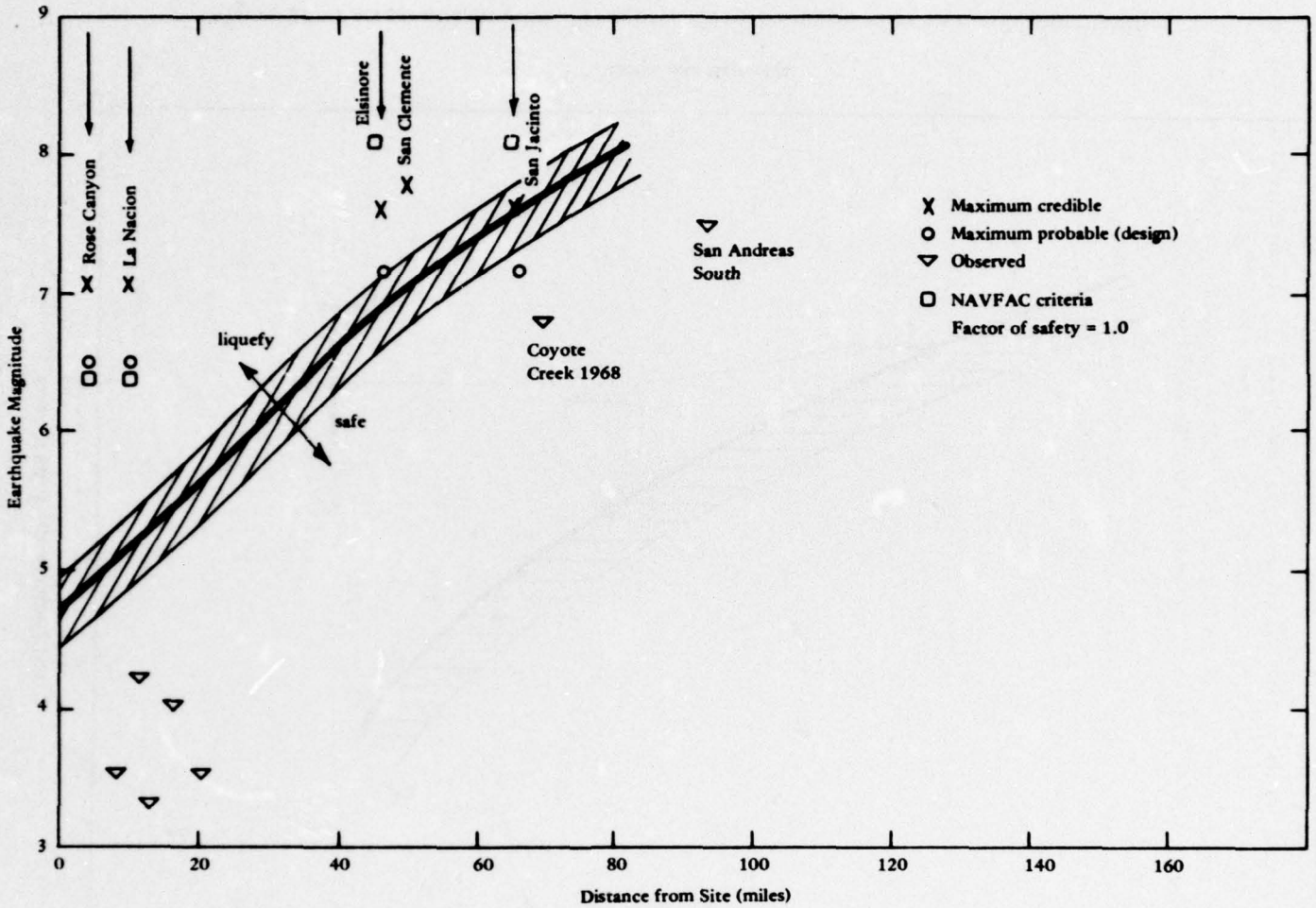

Figure 23. Earthquake magnitude versus distance for liquefaction at NAS North Island.

Direct determination of soil density from recovered drive samples is sometimes carried out; but the validity of this method, based upon density measurements on what must be considered a "disturbed" sample, are of questionable value. The fact that the soil must be essentially cohesionless and must be located beneath the water table for liquefaction to be of concern further limits the value of drive samples used for such purposes.

To estimate absolute in-situ density from the relative-density/blow-count correlations, it is necessary to also know the maximum and minimum possible densities of the material. Thus, in addition to any errors introduced in conducting the penetration tests and to any errors inherent in the available correlation charts used, further errors may be introduced during the laboratory determinations of values of the maximum and minimum possible densities. Since D_r is calculated as the difference between numbers of similar orders of magnitude, even relatively small errors in individual density evaluations can result in considerably large errors in D_r. Reference 49 suggests that typical errors in D_r determinations encompass a spectrum of densities from those depicting improbable liquefaction to those ensuring certain liquefaction under typical design earthquake levels. Thus, although dynamic penetrations are extremely valuable qualitative indicators of foundation competence, they may not provide the precise quantitative information necessary for liquefaction analysis.

As stated previously, available dynamic penetration information at NAS North Island indicated that some of the subsurface soils were extremely soft or loose. These very low penetration resistance values, though consistent, were low enough to cause one to suspect that liquefaction was occurring in advance of the sampler or that some structure or cementation was present which had prevented the in-situ soils from achieving a degree of compaction consistent with the in-situ pressures. The knowledge that very loose soils may be characterized unrealistically weak by dynamic penetration tests [45] increased these suspicions. To avoid the shortcomings of the SPT, which is associated with sample disturbance, it was decided to select a different method of field investigation which could be correlated with the behavior of the soil, in-situ, in an undisturbed state. The friction cone method [7, 8, 50] was chosen for this purpose. Static cone penetration tests are used very extensively in Europe and other parts of the world. This technique was originally developed for evaluation of pile capacities, particularly in sands below the water table, where it is extremely difficult to sample cohesionless soils. This approach was also found to be an accurate indicator of soil density.

The soil information secured with the friction cone (Figure 4) and as interpreted for the former Spanish Bight area (Figure 5), also indicated extremely loose cohesionless deposits existing at North Island. Both the available dynamic penetration testing and the quasi-static cone resistance values suggested granular soils as loose as 15% relative density [44]. In addition, the dynamic penetration tests carried out at the same locations as the friction cone tests showed a remarkable agreement. Nevertheless,

it is very difficult to maintain typical cohesionless soils at densities as low as this, unless perhaps under partially saturated conditions. Furthermore, studies using more sophisticated methods of determining the density of hydraulically placed fills [46, 51] indicated that in-situ relative densities of less than about 40% are generally not encountered below the water table.

The explanation for the anomaly at North Island appears to lie in the peculiar nature of the in-situ soils. The extremely micaceous sandy deposits attain lower densities than normal soils due to the unusual number of flat, flexible platey particles (see Figure 7). The silty bay deposits, that pose the serious liquefaction threat appear to have a degree of cementation that has prevented their consolidating to the extent expected under prevailing conditions. Upon destruction of this cementation, either by the friction cone or the dynamic drive sampler, this material reverts to an extremely unstable state. Unfortunately, the behavior of this unusual material during an earthquake cannot be surmised. The relative density value of 35%, selected to characterize the potentially liquefiable layer, is higher than the densities indicated by empirical correlations with the exploratory data. However, it is considered the lowest reasonable value applicable to typical soils. Since the approach to liquefaction evaluation used herein was developed for typical soils, the D_r value of 35% is considered reasonable. Obviously, a great deal of judgment is required in this regard, and the results must be considered cautiously.

Determination of Liquefaction Potential

After the state of the in-situ soil, particularly with regard to density, ambient stress levels, and soil structure has been identified, and the input ground motions selected, it is then necessary to determine the soil response under specific earthquake input motions. This can be done by using sophisticated cyclic soil testing, assuming suitable facilities are available and properly representative soil specimens can be obtained. As stated previously, drive samples cannot be considered undisturbed, and the reconstruction of samples using density correlations based upon SPT tests must be considered with caution. Cyclic load testing is generally carried out either by means of a simple shear apparatus [36, 37] or by using triaxial tests [32, 35]. Since equipment of the former type is not generally available, most laboratory cyclic testing is conducted using triaxial test apparatus.

Laboratory soil liquefaction criteria are generally presented in the form of a cyclic shear stress level versus the number of cycles of loading to either initial liquefaction or to some arbitrary strain level (see Figure 17). Available data suggest that neither the shapes of the loading pulses nor their frequencies (within a relatively broad range) are particularly important [37, 40]. This is significant. Otherwise, it would be extremely difficult to define an "equivalent" earthquake input for practical laboratory testing.

The treatment of data is further simplified by the observation that cyclic shear stress level can be reasonably normalized in terms of effective initial confining pressures. In addition, it is generally accepted that data obtained on specimens of different densities can be related as inverse functions of the relative density as long as D_r is less than 75% [31]. This means the number of cycles causing liquefaction can be directly related to the dimensionless ratio $\tau/\sigma_c D_r$, as defined previously.

Inherent in this approach is the assumption that the effect of a load cycle having particular characteristics is the same, whether it is accompanied by stress cycles having markedly different amplitudes, and regardless of the sequence in which these cycles are applied. (Unfortunately, data exists [52] which suggests that the sequence of the larger peaks can be of significance regarding the number of cycles to liquefaction.) The approach also assumes no drainage; i.e., no reduction of pore pressure takes place between cycles.

It has been shown [53] that grain size and gradation of cohesionless soils are of secondary importance with respect to liquefaction where no drainage is permitted. This assumption permits a uniform set of criteria to be used throughout a soil profile without corrections for grain size variations.

The foregoing may be valid prior to approaching the liquefaction condition, but the behavior of the soil near liquefaction can be expected to vary markedly as a function of the relative density, and perhaps other soil properties such as angularity and gradation. For example, Reference 54 notes that even under undrained conditions, pore pressures do not build up as high in coarser materials as in finer ones. Following initial liquefaction, denser soils tend to dilate, causing pore water tension and opposing liquefaction. Such soils cannot undergo a permanent loss of strength without some pore waterflow or cavitation of the water. This may be unlikely in the small interstices between grains. Thus, initial liquefaction in dense soils may not be of any practical significance.

Triaxial testing generally is conducted by first consolidating the specimen under a uniform hydrostatic stress, and then subjecting it to an alternating deviator (or vertical) stress, $\pm\tau$. This is equivalent to having a coefficient of lateral earth pressure, k_o, equal to unity during the consolidation stage.

Consolidating the specimen at other values of k_o is not desirable since applied shear stresses do not act upon the horizontal or vertical planes and the shear stress cycles would no longer be applied symmetrically [32]. The shear stress level commonly used in defining failure in the triaxial cell is the maximum shear stress, or one-half the value of the applied deviator stress. This is not the shear stress level on the plane of maximum obliquity, as is the value used for simple shear tests, or as determined for field applications. Furthermore, triaxial testing introduces very large rotations (90 degrees and symmetrical) in the directions of the principal stresses. The intermediate principal stress level also alternates between the value of the maximum and minimum principal stresses as the deviator stress alternates between tension and compression, respectively.

Because of the differences between the laboratory environment and the field, corrections to laboratory results become necessary. A basis for estimating correction factors that are caused by variations of the coefficient, k_o, is presented in Reference 32. This work suggests that laboratory triaxial strength data should be reduced by factors of about one-half to account for the lower k_o conditions existing in the field. On the other hand, disturbances to laboratory specimens and limitations in testing equipment are considered capable of reducing laboratory strength results by 15 to 50% below field values. To derive a valid correction factor encompassing all the variations between laboratory and field liquefaction, Reference 32 compares field and laboratory liquefaction histories. Using estimated values of maximum accelerations generated at various sites by previous earthquakes and normalizing all field results to a relative density, D_r, of 50%, comparisons between laboratory failure predictions and actual field failures are made. On this basis correction factors have been developed for correcting laboratory triaxial data to make is representative of field conditions. This study [32] indicates reasonable agreement between correction factors based on analytical studies and those derived from field comparisons. These comparisons involved placing numerical values on laboratory test shortcomings and estimating peak shear stress in the field on the basis of deduced earthquake magnitudes. Also, for these comparisons, relative densities of the soils in the field were based upon standard penetration test results. More recent work [55] based upon shake-table tests has suggested correction factors for triaxial tests of about the same magnitude.

In addition to using laboratory procedures to depict the onset of initial liquefaction, they may also be used to define the number of stress cycles that will result in specific levels of strain deformation in the field. Since initial liquefaction presumes reduction of effective stress to zero, continued triaxial cycling results in an attempt to generate shear stress loadings by application of tensile stresses to the soil particles. Such a loading mechanism cannot be expected to simulate field loading, particularly as large deformations commence. This is perhaps why Finn, et al, [37] note that the alternating pore pressure levels so characteristic of triaxial tests prior to failure are not so prevalent in simple shear tests.

Various other factors influence the proper selection of appropriate liquefaction criteria from laboratory tests. Although, for example, the gradation appears to be of secondary importance under undrained conditions, it is known to be extremely important in actual field cases, as indicated by experience during the Alaskan earthquake of 1964. During that earthquake, structures founded on coarse materials behaved considerably better than those located over finer deposits [53].

The effect of in-situ lateral stress is known to be very important [32], but evaluation of this stress level in the field is extremely difficult. Previous history can markedly reduce the potential for liquefaction [56], but a detailed stress history for in-situ soil deposits can never be known with any certainty. Thus, current approaches to liquefaction prediction are fraught with many difficulties.

Considering the possible errors involved in the correction factors applied to triaxial test data, it is questionable whether actual cyclic testing, even having truly undisturbed samples and using refined test apparatus, is any more reliable than using published data such as that presented in Figure 17. Nevertheless, an orderly approach to liquefaction analysis now exists where formerly there was none. The only serious criticism of this procedure is that it simplifies a very complex problem to the extent that it is easy to come up with liquefaction evaluations which, while appearing to be rigorously carried out, could still be grossly in error. For example, the materials at North Island can be expected to depart dramatically from the normal situation, as inherently assumed in the development of the approach used for this liquefaction analysis. Thus, much judgment must be used in applying this type of analysis to actual field situations.

RESULTS

The major portions of NAS North Island are underlain by natural sands which should be fairly resistant to liquefaction. However, based upon previous foundation investigations and the soil investigations and liquefaction analysis conducted during this study, regions of high risk from liquefaction at NAS North Island have been located. Two such regions, where soft cohesionless materials exist below the water table (see Figure 1), were located. One of these areas—over the former Spanish Bight (Region I)—consists of an area of land roughly 2,000 feet wide, extending about 1/2 mile in the south-southwest direction from the carrier docking facilities (and generally following along the eastern side of Wright Avenue). The second critical area with respect to liquefaction (Region II) is located in the filled region along the northwest margin of the air station (west of Taxiway No. 5). The scope of this project did not include extensive detailed soil borings to define the boundaries of these regions.

The numerical results of the analysis are best illustrated by Figure 23, which shows the range at which liquefaction will occur for earthquakes of given magnitudes. The region investigated (Region I) has a factor of safety of less than 1.0 for earthquakes 6.9 or greater on the Elsinore fault and 4.7 or greater on the Rose Canyon fault (see Figure 1). Of particular significance is the fact that the Rose Canyon fault should be considered as active and capable of producing an earthquake of importance to the site. Thus, available information predicts that liquefaction will occur within Regions I and II at North Island under predictable earthquake levels, particularly upon either the Elsinore, La Nacion, or Rose Canyon faults.

In the event of such an earthquake, liquefaction in the vicinity of load discontinuities could cause sand blows and waterspouts at the surface. In areas where the land slopes or embankments are present, significant flow displacements of 5 feet or more could occur, depending upon the duration of the strong motion and the in-situ drainage situation. Even in the absence of large lateral movements, consolidations

of the softer sediments could cause surface settlements of up to a foot. Soil areas experiencing high shear stresses such as those located under heavy structures could undergo both displacement and rotation.

A detailed analysis of individual structures is outside the scope of this report; however, the following comments are offered:

Region I – If the liquefiable layers are continuous over this region, large ground motions could occur. The magnitude of the dislocations at the carrier docking facilities would depend somewhat upon the types of static loads being applied to the dock areas at the time of the earthquake. If the period of liquefaction should coincide with other events, such as drawdown of the seawater level in the harbor due to a tsunami, very large movements of the docks and moored vessels would be expected. With the exception of several water tanks located in Region I, most structures appear to be primarily warehouses and other noncritical structures. However, the main water and sewer lines and other critical services to the Naval Air Station pass through this region and would be destroyed if large ground movements occurred.

Region II – This region was not analyzed in detail because of the limited soil input data available; however, this region would be expected to behave like Region I. On the basis of the data obtained, this area would also undergo liquefaction under design earthquake levels. If these potentially liquefiable deposits should extend under an adjacent aviation gasoline tank farm, an extremely high fire risk might occur from rupture and leakage of the tanks.

RECOMMENDATIONS

Based upon this study, the following are recommended:

1. Effort should be made to define more precisely the boundaries of the potentially liquefiable areas noted as Regions I and II.

2. Detailed evaluations of possible movements should be conducted for any critical structures, including carrier docks located near liquefiable deposits. Based upon these findings, remedial measures can be designed and taken as necessary.

3. All main utility service lines passing through or over potentially liquefiable deposits should be relocated, or alternate routes for supplying critical services following an earthquake should be established.

4. Plans for new construction at North Island should be re-evaluated to insure that such construction is not sited within potentially liquefiable areas.

5. Detailed geologic investigation should be performed to locate the Rose Canyon fault on North Island and to provide better definition of the soil and rock at depths.

6. No significant structure should be located within 100 feet of the determined fault line.

7. Liquefaction evaluations should be conducted at other naval installations to establish patterns or provide comparative evaluations of liquefaction risks. With the continued occurrence of earthquakes, this would provide improved reliability for hazard prediction levels.

8. Improved undisturbed sampling techniques such as those encompassing soil freezing, chemical injection, or initial dewatering should be used where precise evaluation of liquefaction is necessary.

9. Efforts should be initiated to develop in-situ liquefaction evaluation procedures which would avoid the major difficulties of sampling and laboratory testing.

REFERENCES

1. Office of Naval Research. General review of the seismic hazard to selected U.S. Navy installations, by ONR Natural Hazards Review Panel. Washington, DC, Jan 1974.

2. M. P. Kennedy. Bedrock lithologics, San Diego coastal area, California. Studies of the geology and geologic hazards of the greater San Diego areas, California. San Diego, CA, San Diego Associations of Geologists and Engineering Geologists, May 1973.

3. California Division of Mines and Geology. County Report 3: Mines and mineral resources of San Diego County, California. San Francisco, CA, 1973.

4. San Diego Planning Department, prepared by Woodward-Gizienski and Associates. Seismic safety study for the city of San Diego, San Diego, CA, Aug 1974.

5. J. H. Schmertmann. "Static cone penetrometers for soil exploration," Civil Engineering, vol 37, no. 6, June 1967, pp 71-73.

6. G. F. A. Fletcher. "Standard penetration test: its uses and abuses," Journal of the Soil Mechanics and Foundations Division, ASCE, vol 91, no. SM4, Jul 1965, p. 75. (PWC Paper 4395)

7. Army Corps of Engineers, Waterways Experiment Station. Contract Report 5-69-4: Dutch friction cone penetrometer exploration of research area at Field 5, Eglin AFB, Florida, by J. H. Schmertmann. Vicksburg, MS, Oct 1969.

8. G. Sanglerat. The penetrometer and soil exploration, tr. by G. Gendarme. Amsterdam, The Nethlerlands, Elserier Publishing Co., 1972.

9. G. G. Meyerhof. "Penetration tests and bearing capacity of cohesionless soils," Journal of the Soil Mechanics and Foundations Division, ASCE, Jan 1956. (PWC Paper 866, SM1)

10. T. H. Wu. Soil mechanics. Boston, MA, Allyn and Bacon, Inc., 1966.

11. T. Atwater. "Implications of plate tectonics for the Cenozoic tectonic evolution of western North America," Geological Society of America Bulletin, vol 81, 1970.

12. B. Guttenberg and C. F. Richter. Seismicity of the Earth, 2nd ed. Princeton, NJ, Princeton University Press, 1956.

13. Association of Engineering Geologists. Geological Severity and Environmental Impact Special Publication: Recency of faulting in the greater San Diego area—California, by J. I. Ziony. Los Angeles, CA, University Publishers, Oct 1973.

14. C. M. Wentworth and R. F. Yerkes. "Geologic setting and activity of faults in the San Fernando area, California," in The San Fernando, California, Earthquake of February 9, 1971, U. S. Geological Survey Professional Paper 733, Washington, DC, 1971, pp 6-16.

15. Department of Interior, Geological Survey. Preliminary Report: Recency of faulting in the greater San Diego Area, by Z. I. Ziony and D. M. Buchanan. Washington, DC, 1972.

16. D. Tocher. "Earthquake energy and ground breakage," Seismological Society of America Bulletin, no. 48, 1958, pp 147-153.

17. C. King and L. Knopoff. "Stress drop in earthquakes," Seismological Society of America Bulletin, vol 58, no. 1, 1968, pp 249-257.

18. M. G. Bonilla. "Chapter 3, Surface faulting and related effects," Earthquake Engineering, edited by Robert L. Wiegel. Englewood Cliffs, NJ, Prentice-Hall, Inc., 1970.

19. Dames and Moore. Engineering Bulletin no. 46: Earthquake hazards for buildings, by N. C. Donovan. Los Angeles, CA.

20. H. B. Seed, I. M. Idriss, and F. W. Kiefer. "Characteristics of rock motions during earthquakes," Journal of the Soil Mechanics and Foundations Division, ASCE, vol 95, no. SM 5, Sep 1969, pp 1199-1218.

21. Association of Engineering Geologists. Geologic, Seismicity and Environmental Impact Special Publication: Earthquake recurrence intervals on major faults in southern California, by D. L. Lamar, P. M. Merifield, and R. J. Proctor. Los Angeles, CA, University Publishers, Oct 1973.

22. U. S. Geological Survey. Professional Paper 800 C: Offshore extension of the Rose Canyon fault, San Diego, California, geological survey research, by G. Moore. Washington, DC, 1972, pp C113-C116.

23. R. B. McEuen and C. J. Pinckney. "Seismic risk in San Diego," in Transactions of the San Diego Society of Natural History, vol 17, no. 4, Jul 1972.

24. P. B. Schnabel and H. B. Seed. "Accelerations in rock for earthquakes in the western United States," in Bulletin of the Seismological Society of America, vol 63, no. 2, 1973, pp 501-516.

25. California Division of Mines and Geology. Map Sheet 23: Maximum credible rock accelerations from earthquakes in California, by R. W. Greensfelder. Sacramento, CA, 1974.

26. California Institute of Technology, Seismological Laboratory. Seismicity of the southern California region, 1 January 1932 to 31 December 1972, by J. A. Hileman, C. R. Allen, and J. M. Nordquist. Pasadena, CA, 1973.

27. University of California, Earthquake Engineering Research Center. Report no. EERC 72-12: SHAKE, a computer program for earthquake response analysis of horizontally layered sites, by P. B. Schnabel, J. Lysmer, and H. B. Seed. Berkeley, CA, Dec 1972.

28. University of Kentucky, College of Engineering. Technical Report UKY 26-70-CE 2: Shear modulus and damping in soils, I. Measurement and parameter effects, soil mechanics series no. 1, by B. O. Hardin and V. P. Drnevich. Lexington, KY, Jul 1970.

29.——. Technical Report UKY 26-70-CE 3: Shear modulus and damping in soils, II. Design equations and curves, soil mechanics series no. 2, by B. O. Hardin and V. P. Drnevich. Lexington, KY, Jul 1970.

30. I. M. Idriss, H. B. Seed, and N. Serff. "Seismic response by variable damping finite elements," Journal of the Geotechnical Engineering Division, ASCE, vol 100, no. GT1, Jan 1974. (Proc. Paper 10284).

31. H. B. Seed, J. Lysmer, and R. Hwang. "Soil structure interaction analysis for seismic response," Journal of the Geotechnical Engineering Division, ASCE, vol 101, no. GT5, May 1975. (Proc. Paper 11318)

32. H. B. Seed and W. H. Peacock. "Test procedure for measuring soil liquefaction characteristics," Journal of the Soil Mechanics and Foundations Division, ASCE, vol 97, no. SM8, Aug 1971.

33. S. W. Nunnally. Development of a liquefaction index for cohesionless soils, Ph D thesis, Northwestern University. Evanston, IL, 1965.

34. K. L. Lee. "Number of equivalent significant cycles in strong motion earthquakes," in Proceedings of International Conference on Microzonation, vol 2, Seattle, WA, Oct 1972.

35. H. B. Seed and K. L. Lee. "Liquefaction of saturated sands during cyclic loading," Journal of the Soil Mechanics and Foundations Division, ASCE, vol 92, no. SM6, Nov 1966. (Proc. Paper 4972)

36. W. H. Peacock and H. B. Seed. "Sand liquefaction under cyclic loading simple shear conditions," Journal of the Soil Mechanics and Foundations Division, ASCE, vol 94, no. SM3, May 1968.

37. W. D. L. Finn, D. J. Pickering, and P. L. Bransby. "Sand liquefaction in triaxial and simple shear tests," Journal of the Soil Mechanics and Foundations Division, ASCE, vol 97, no. SM4, Apr 1971.

38. I. Ishibashi and M. A. Sherif. "Soil liquefaction by torsional simpel shear device," Journal of the Geotechnical Engineering Division, ASCE, vol 100, no. GT8, Aug 1974. (Proc. Paper 10752)

39. H. B. Seed and I. M. Idriss. "Simplified procedure for evaluating soil liquefaction potential," Journal of the Soil Mechanics and Foundations Division, ASCE, vol 97, no. SM9, Sep 1971.

40. N. C. Donovan. "A stochastic approach to the seismic liquefaction problem," in Proceedings of the First International Conference on Applications of Statistics and Probability to Soil and Structural Engineering, Hong Kong, Sep 1971. Hong Kong, Hong Kong University Press, 1972.

41. California Institute of Technology. Miscellaneous Report SEM-68: Simulated earthquake motions, by P. C. Jennings, G. W. Hausner, and N. C. Tsai. Pasadena, CA, Apr 1968.

42. H. B. Seed. "Design procedures for assigning the effects of local geology and soil conditions on ground and building response due to earthquakes, chapter 6." Proceedings of Earthquake Symposium, Structural Engineers Association of Southern California, Los Angeles, CA, Jun 1975.

43. City of San Diego. Seismic safety element. San Diego, CA, Aug 1974.

44. H. J. Gibbs and W. G. Holtz. "Research on determining the density of sand by spoon penetration testing," in Proceedings of the Fourth International Conference of Soil Mechanics and Foundation Engineering, vol 1, 1967, p. 35.

45. A. R. S. Bazaraa. Use of the standard penetration test for estimating settlements of shallow foundations on sand, Ph D thesis, Civil Engineering, University of Illinois. Urbana, IL, 1967.

46. J. O. Osterberg and S. Varaksin. "Determination of relative density of sand below ground water table," American Society for Testing and Materials, STP 523. Philadelphia, PA, Jun 1972, pp 364-378.

47. F. A. Tavenas and P. LaRochelle. "Accuracy of relative density measurements," Geotechnique, vol 22, no. 4, 1972.

48. H. A. Mohr. "Discussion to 'Standard penetration test: its uses and abuses, by G. F. A. Fletcher,' " Journal of the Soil Mechanics and Foundations Division, ASCE, vol 92, no. SM1, Jan 1966, p. 196.

49. F. A. Tavenas. "Discussion to 'Simplified procedure for evaluating soil liquefaction potential, by H. B. Seed and I. M. Idriss,' " Journal of the Soil Mechanics and Foundations Division, ASCE, Vol 98, no. SM4, Apr 1972, p. 433.

50. Proceedings of the European symposium on penetration testing, vol 1. Stockholm, Sweden, Swedish Geotechnical Society, Jun 1974.

51. R. V. Whitman. "Hydraulic fills to support structural loads," Journal of the Soil Mechanics and Foundations Division, ASCE, vol 96, no. SM1, Jan 1970.

52. K. Ishihara and S. Yasuda. "Sand liquefaction under random earthquake loading condition," in Proceedings of Fifth World Conference on Earthquake Engineering. Rome, Italy, June 25-29, 1973, pp 329-339.

53. University of California, Earthquake Engineering Research Center. Report No. EERC 74-11: Liquefaction of gravelly soils under cyclic-loading conditions," by R. T. Wong, H. B. Seed, and C. K. Chan. Berkeley, CA, Jun 1974.

54. K. L. Lee and J. A. Fitton. "Factors affecting the cyclic loading strength of soil," Vibration Effects of Earthquakes on Soils and Foundations, ASTM STP no. 450. Philadelphia, PA, 1969, pp 71-95.

55. University of California, Earthquake Engineering Research Center. Report No. EERC 75-14: Determination of soil liquefaction characteristics by large-scale laboratory tests, by P. De Alba, C. K. Chan, and H. B. Seed. Berkeley, CA, May 1975.

56. K. L. Lee and J. A. Focht. "Liquefaction potential at Ekofisk tank in North Sea," Journal of the Geotechnical Engineering Division, ASCE, vol 101, no. GT1, Jan 1975. (Proc. Paper 11054)

Appendix

SOIL INVESTIGATIONS AT NAS NORTH ISLAND

Number[a]	Project Title	Report Date	Originator
1	San Diego Gas and Electric Station	1-75	Woodward-Gizienski and Associates
2	AIMD Airframe Shop P-334	7/31/74	Woodward-Gizienski and Associates
3	Proposed BEQ P-193	2/25/72	Woodward-Gizienski and Associates
4	Aircraft Systems Training Building (P-364) NAS, North Island, San Diego, CA	5/3/74	Woodward-Gizienski and Associates
5	Soil Investigation, Proposed Building P-107	9-68	Woodward-Clyde and Associates
6	Soil Investigation, Proposed 2-Story Apartment Building	1-70	Woodward-Clyde and Associates
7	Final Report Foundation Investigation Proposed Ammunition Pier	9/30/74	Dames and Moore
8	Results of Soil Investigation at Chemical Disposal Site, US NAS North Island, CA	5-72	Civil Engineering Laboratory, NCBC
9	Pile Capacities, Proposed Turbo-Jet Engine Test Cells	2-54	L. T. Evans, Engineer
10	Foundation Investigation, Proposed Addition to Boiler Plant Building	5-68	LeRoy Crandall and Associates
11	Proposed Taxiway Site	9/27/73	Southern California Test Laboratory
12	Soils Investigation, Construction of Collimation Tower and Antenna Array	1-63	Benton Engineers, Inc.
13	Foundation Investigation, Proposed Turbo-Jet Engine Test Facility	5-57	Donald R. Warren

[a]Numbers refer to locations in Figure 3.

Number[a]	Project Title	Report Date	Originator
14	Proposed Engine Parts Coating Facility (P-143) NAS, North Island, CA	4/16/74	Benton Engineers, Inc.
15	Foundation Investigation, Oxygen and CO_2 Bottle Testing, Overhaul and Charging Building	8-54	L. T. Evans, Engineer
16	Soils Investigation, Proposed Maintenance Hangar	8-62	Woodward-Clyde-Sherard and Associates
17	Foundation Investigation, Proposed Operations Control Center, Building no. 93	7-62	Dames and Moore
18	Soil Investigation, Proposed Radar Buildings	6-70	Woodward-Clyde and Associates
19	Bachelor Enlisted Quarters (BEQ) P-193, Site 2	1/31/73	Woodward-Gizienski and Associates
20	Soils Investigation, Mess Hall/Connecting Building 317 (P-031)	6-71	Southern California Testing Laboratory Inc.
21	Soils Investigation, Training Building for P3V-1 and W2F-1 Maintenance Trainers	4-62	Benton Engineers, Inc.
22	Soils Report, Aircraft Systems Training Building (P-075)	7-67	Woodward-Clyde-Sherard and Associates
23	Soil Investigation for the Proposed Barracks Building P-021, 2nd Increment	4-67	Woodward-Clyde-Sherard and Associates
24	Soil Investigation, Navy Exchange Building	1-68	LeRoy Crandall and Associates
25	Proposed S-3A Training Building (P-304)	5/1/72	Woodward-Gizienski and Associates
26	Foundation Investigation, Helicopter Rotor Blade Test Stand	7-75	LeRoy Crandall and Associates

[a]Numbers refer to locations in Figure 3.

Number[a]	Project Title	Report Date	Originator
27	Aircraft Maintenance Hangar P-225 S.D.	7/25/74	Woodward-Gizienski and Associates
28	Foundation Soils Investigation at NAS North Island	10/3/74	GEO-EKTA Laboratory
29	Hangar Additions and Alterations P-335, N. I.	6/20/74	Woodward-Gizienski and Associates
30	Foundation Investigation, Proposed AUW Shop	4-57	LeRoy Crandall and Associates
31	Soils Investigation, Avionics and Training Facilities, Hangar Building 340	7-63	Benton Engineers, Inc.
32	Foundation Investigation, Fleet Airborne Electronics Training Unit, Pacific (FAETUPAC) Facility	10-55	LeRoy Crandall and Associates
33	Soil Investigation, Proposed Landing Cable Anchors	1-65	Woodward-Clyde-Sherard and Associates
34	Soils Investigation, Aircraft Emergency Repair Facility	7-63	Benton Engineers, Inc.
35	Soil Investigation for Proposed Maintenance Shop and Holding Shed	1/21/75	Woodward-Clyde and Associates
36	Foundation Investigation, Special Weapons Training Facility	8-55	LeRoy Crandall and Associates
37	Foundation Investigation, Proposed Shop Building	4-55	San Diego Testing Laboratory
38	Soil Investigation, Proposed Fuel Storage and Distribution Facilities NAS/N 24-3 (86)	4-57	San Diego Testing Laboratory
39	Repair and Ground Check Development Activity (FY 1958)	4-58	Murray Erick Associates
40	Foundation Investigation, Special Weapons Training Facility	10-55	LeRoy Crandall and Associates

[a]Numbers refer to locations in Figure 3.

Number[a]	Project Title	Report Date	Originator
41	Foundation Investigation, RAMIS Facility	3-57	L. T. Evans, Engineer
42	Soils Investigation, Construction of Magazines	5-57	Benton Engineers, Inc.
43	Soil Investigation for the Proposed Flight Control and Rescue Facility	4/17/72	Woodward-Gizienski and Associates
44	Soils Investigation, Rescue Unit Home Port Facility (P-150)	4-71	Benton Engineers, Inc.
45	Soil Investigation, Proposed Aircraft Parking Apron, Project 0675	8-62	Woodward-Clyde-Sherard and Associates
46	Parking Apron Pavement Replacement/ Vicinity of Hangar 525 and 526	3/29/74	Geocon
47	Soil Investigation, Proposed Transportation Facility	9-52	San Diego Testing Laboratory
48	Foundation Investigation, Proposed Aircraft Accessory Overhaul Facility P-108	2-69	LeRoy Crandall and Associates
49	Preliminary Soil Investigation, Proposed Barracks Building	8-65	Woodward-Clyde-Sherard and Associates
50	Soil Investigation, Operations Building and Transportation Building	11-51	San Diego Testing Laboratory
51	Soil Investigation, Proposed North Island Industrial Waste System	7-69	Woodward-Clyde and Associates
52	Proposed Wastewater Collection at Ship Berths	6/20/72	Boyle Engineering
53	Applied Instrument Building, Addition to Building 335	8/30/73	Benton Engineering
54	Foundation Investigation, Proposed Aircraft Overhaul Facility P-110	10-69	LeRoy Crandall and Associates

[a]Numbers refer to locations in Figure 3.

Number[a]	Project Title	Report Date	Originator
55	Soil Investigation, BOQ Building	11-51	San Diego Testing Laboratory
56	Soil Investigation, Seaplane Beaching Facility	11-54	L. T. Evans, Engineer
57	Foundation Investigation, Overhaul Hangar	1-52	L. T. Evans, Engineer
58	Aircraft Power Check Facility	11-72	Advanced Foundation Engineers, Inc.
59	Soils Investigation, Proposed Aircraft Maintenance Hangar	6-67	Benton Engineers, Inc.
60	Soils Investigation, Proposed Avionics Facilities (P-106)	9-68	Benton Engineers, Inc.

[a]Numbers refer to locations in Figure 3.

DISTRIBUTION LIST

SNDL Code	No. of Activities	Total Copies	
—	1	12	Defense Documentation Center
FKAIC	1	10	Naval Facilities Engineering Command
FKNI	6	6	NAVFAC Engineering Field Divisions
FKN5	9	9	Public Works Centers
FA25	1	1	Public Works Center
—	6	6	RDT&E Liaison Officers at NAVFAC Engineering Field Divisions
—	279	280	CEL Special Distribution List No. 15 for persons and activities interested in reports on Structural Mechanics